

1 A comparative study of the *in vitro* permeation of 2-
2 phenoxyethanol in the skin PAMPA model and mammalian skin

3 Annisa Rahma^{a,b,*}, Majella E. Lane^b, Bálint Sinkó^c

4 ^a School of Pharmacy, Institut Teknologi Bandung, Ganesa 10, Bandung 40132, Indonesia

5 ^b School of Pharmacy, University College London, 29 – 39 Brunswick Square, London WC1N 1AX,
6 United Kingdom

7 ^c Pion Inc., 10 Cook Street, Billerica, Massachusetts 01821, United States

8

9 * corresponding author

10

11 Email addresses: annisarahma@fa.itb.ac.id (A. Rahma), m.lane@ucl.ac.uk (M.E. Lane),

12 bsinko@pion-inc.com (B. Sinkó).

13 **Abstract**

14 For permeation studies that use excised skin, experimental data may show variability
15 associated with the use of biological tissues. As a consequence, achieving reproducible
16 results and data interpretation may be challenging. The skin parallel artificial membrane
17 permeability assay (skin PAMPA) model has been proposed as a high-throughput tool for
18 predicting skin permeation of chemicals. A number of skin cleansing wipe formulations for the
19 diaper area of infants contain 2-phenoxyethanol (PE) as a preservative and cetylpyridinium
20 chloride (CPC) as a surfactant with antimicrobial activity. However, information regarding
21 cutaneous absorption of PE and CPC in the scientific literatures is remarkably limited. The
22 main aim of the present study was to assess the suitability of the skin PAMPA model for
23 prediction of skin permeation of PE. A secondary aim was to investigate the influence of CPC
24 on the dermal absorption of PE. PE (1% w/w) was prepared in two vehicles, namely propylene
25 glycol (PG) and water-PG (WP). Permeability of PE was investigated *in vitro* using the skin
26 PAMPA membrane, porcine skin and human skin under finite dose conditions. The highest
27 permeation of PE was observed for the water-PG preparation with 0.2% w/w of CPC. This
28 finding was consistently observed in the skin PAMPA model and in Franz cell studies using
29 porcine skin and human skin. Permeation of CPC was not detected in the three permeation
30 models. However, permeation of PE increased significantly ($p < 0.05$) in the presence of CPC
31 compared with formulations without CPC. When comparing the skin PAMPA data and the
32 mammalian skin data for the cumulative amount of PE permeated, the r^2 values for PAMPA-
33 porcine skin and PAMPA-human skin were 0.84 and 0.89, respectively. The findings in this
34 study demonstrate the capability of the skin PAMPA model to differentiate between various
35 doses and formulations and are encouraging for further applications of this model as a high
36 throughput screening tool in topical formulation development.

37 **Keyword:** dermal absorption, PAMPA, porcine skin, human skin, preservative, surfactant.

38

39 **1. Introduction**

40 Dermal absorption of ingredients in topical formulations intended for infants has not been
41 widely studied. The importance of assessing skin permeation of such ingredients has recently
42 been reviewed (Rahma and Lane, 2022; Stamatias et al., 2021). Baby wipes are used regularly
43 in the infant population, and mainly comprise a high percentage of water (>90%),
44 preservative(s), and surfactant(s). Phenoxyethanol (PE) is the most commonly used
45 preservative ingredient in baby wipe formulations and is typically included at a concentration
46 of 0.5-1% w/v. PE has been shown to demonstrate significantly lower adsorption ($p < 0.05$) to
47 the fabric component of baby wipes in comparison with methylparaben (Endo et al., 2020). In

48 addition, PE (log P 1.2) has a comparatively higher aqueous solubility compared with other
 49 preservatives commonly used in topical preparations such as parabens and benzoic acid
 50 (Sheskey et al., 2020). These are important considerations for formulations with high water
 51 content such as baby wipes. Although PE is extensively used in baby wipe formulations
 52 (Salama et al., 2021), it has also been reported to act as a penetration enhancer (Ibrahim and
 53 Li, 2009; Ibrahim and Li, 2010). The haemolytic effects of PE have long been acknowledged
 54 (European Union Scientific Committee on Consumer Safety, 2016). Following oral
 55 administration, PE undergoes rapid first pass metabolism and is then converted into 2-
 56 phenoxyacetic acid (European Union Scientific Committee on Consumer Safety, 2016).
 57 Therefore, the systemic bioavailability of PE is very low (European Union Scientific Committee
 58 on Consumer Safety, 2016). By contrast, percutaneous absorption resulted in higher
 59 concentrations of PE in blood (Kim et al., 2015). In 2012, the French National Agency for the
 60 Safety of Medicines and Health Products (ANSM) submitted a risk assessment concerning
 61 the use of PE as a preservative ingredient in cosmetic formulations (French National Agency
 62 for the Safety of Medicines and Health Products, 2019). The ANSM proposed that PE should
 63 be excluded from topical formulations intended for the diaper area of infants and children aged
 64 under 3 years. The main reasons were the haematotoxicity and hepatotoxicity potential and
 65 insufficient margins of safety (MoS) for children under 3 years old (Dreno et al., 2019;
 66 European Union Scientific Committee on Consumer Safety, 2016).

67 Some baby wipe formulations also contain cetylpyridinium chloride (CPC), a quaternary
 68 surfactant with antimicrobial activity. For example, three commercial baby wipes listed in Table
 69 1 contain PE and CPC. To date there is no information in the published scientific literature
 70 regarding the skin permeation of PE in the presence of surfactant(s). Although several authors
 71 have reported skin permeation of PE these studies used rodent skin. Therefore, the
 72 experimental data cannot be extrapolated to humans (Lane, 2013).

73
 74 Table 1. Commercial baby wipes containing PE and CPC

75

<u>Ingredient list</u>	<u>Cussons baby wipes pure & gentle</u>	<u>Paseo baby wipes</u>	<u>Pigeon baby wipes</u>
<u>Water</u>	* -	* -	* -
<u>PE</u>	* -	* -	* -

<u>PG</u>	*	*	
	-	-	
<u>Polyhexamethylene biguanide</u>		*	
		-	
<u>Benzalkonium chloride</u>			*
			-
<u>CPC</u>	*	*	*
	-	-	-
<u>Croduret</u>		*	
		-	
<u>PEG-40 hydrogenated castor oil</u>	*		
	-		
<u>PPG-5-ceteth-20</u>	*		
	-		
<u>Sodium lactate</u>	*		
	-		
<u>Sodium citrate</u>			*
			-
<u>Citric acid</u>		*	*
		-	-
<u>Sodium benzoate</u>			*
			-
<u>Disodium EDTA</u>	*		
	-		
<u>PEG-45 palm kernel glycerides</u>	*		
	-		
<u>Sodium lauryl sarcosinate</u>	*	*	
	-	-	
<u>Olea europaea fruit oil</u>	*		
	-		
<u>Cyclodextrin</u>	*		
	-		
<u>Methylparaben</u>	*		
	-		
<u>l-menthol</u>	*		
	-		
<u>Ethylparaben</u>	*		
	-		
<u>Butylparaben</u>	*		
	-		
<u>Propylparaben</u>	*		
	-		
<u>Polydimethylsiloxane</u>	*		
	-		
<u>Chamomile extract</u>		*	
		-	

Perfume

*

Prunus serrulata

*

flower extract

-

76

77 Excised human skin is the most preferred tissue for *in vitro* skin permeation studies that
78 are intended to estimate results in human (Dick and Scott, 1992; Schmook et al., 2001). The
79 major challenges in using excised human skin are (1) difficulty in sourcing the skin samples
80 and (2) intra- and inter-specimen variability (Dick and Scott, 1992; Schmook et al., 2001). The
81 latter may also be problematic when interpreting the results from permeation studies (Oliveira
82 et al., 2010; Zhang et al., 2019). Porcine skin has been considered as an appropriate surrogate
83 for human skin, with reference to the close representation of the permeability properties of
84 porcine tissue to human skin compared to other animal models (Dick and Scott, 1992;
85 Schmook et al., 2001). However, porcine skin reportedly has a lower barrier function than
86 human skin (Barbero and Frasch, 2009; Schmook et al., 2001; Yoshimatsu et al., 2017). In
87 addition, ethical concerns over the use of animals in experiments is rising (Hopf et al., 2020;
88 Pistollato et al., 2021). In light of these challenges, there has been a growing interest in
89 exploring high throughput permeation models that are capable of generating reproducible data
90 that may be extrapolated to man (Zhang et al., 2019).

91 The skin Parallel Artificial Membrane Permeation Assay (PAMPA) model has been
92 developed for prediction of percutaneous absorption. The development of the skin PAMPA
93 membrane and its use as percutaneous absorption model was first described by Ottaviani et
94 al. (Ottaviani et al., 2006). The membrane composition was then refined by Sinkó et al. to
95 achieve better representation of the intercellular stratum corneum (SC) region (Sinkó et al.,
96 2012). The skin PAMPA membrane is essentially a filter substrate coated with synthetic lipids
97 (ceramides, free fatty acids, and cholesterol) arranged in a 96-well plate. Several studies
98 have reported positive correlations for the permeability parameters of compounds using the
99 skin PAMPA model and conventional *ex vivo* permeation studies (Balázs et al., 2016; Kovács
100 et al., 2021; Sinkó et al., 2021; Zhang et al., 2019). However, these studies only investigated
101 permeation of actives under infinite dose conditions.

102 It is important to assess skin permeation using clinically relevant doses, where the applied
103 dose represents the actual exposure “in use”. Clinically relevant doses demonstrated a finite
104 dose profile or “plateau” for *in vitro* permeation studies (Franz, 1975, 1983; Lehman, 2014).
105 This reflects the depletion of the applied dose of active over time (Franz, 1983; Lehman, 2014).
106 Most recently Zhang and co-workers reported that permeation data for niacinamide in the skin

107 PAMPA model correlated well with porcine and human skin *in vitro* studies under finite dose
108 conditions but not under infinite dose conditions (Zhang et al., 2019). Thus, the primary
109 objective of the present work was to investigate the suitability of the skin PAMPA model for
110 determination of dermal absorption of PE in the presence and absence of CPC in model
111 formulations. To this end, *in vitro* studies were conducted in the skin PAMPA model and in
112 porcine skin or human skin using Franz diffusion cells under finite dose conditions. A
113 secondary objective was to elucidate the influence of CPC on the dermal absorption of PE.

114

115 **2. Materials and Methods**

116 **2.1. Materials**

117 PE, CPC, and propylene glycol (PG) were purchased from Sigma-Aldrich Co., USA. HPLC
118 grade solvents (acetonitrile, methanol, water, and trifluoroacetic acid) were purchased from
119 Fischer Scientific, UK. Phosphate-buffered saline (PBS) tablets were purchased from Oxoid
120 Ltd., UK. Porcine ear skin was obtained from a local abattoir. Excised abdominal human skin
121 from a single donor was obtained from a tissue bank with informed consent and institutional
122 ethical approval (Research Ethics Committee reference 07/H1306/98). Skin specimens were
123 stored at -20 °C prior to use. The skin PAMPA sandwich plate, skin PAMPA collector plates,
124 standard hydration solution, stirring disks and Gut-Box™ were supplied by Pion Inc. Billerica,
125 USA.

126

127 **2.2. Methods**

128 **2.2.1. Preparation of test solutions**

129 PE solutions were prepared in the presence or absence of CPC, as shown in Table [42](#).
130 PG was chosen as a single solvent system, whereas water-PG [97:3](#) (WP) was chosen as a
131 vehicle that better represents the cleansing liquid in baby wipes. In addition, selected
132 formulations contained CPC either at 0.2% (w/w) or 1% (w/w). These concentrations represent
133 the typical concentration of surfactants used in baby wipes (Cunningham et al., 2008;
134 Cunningham et al., 2016; Sheehan, 2016). The full details of the formulations used in this
135 study are listed in Table [42](#).

136

137 **Table [42](#).** PE solutions used in permeation studies.

Formulation	PE (% w/w)	CPC (% w/w)	Vehicle
PG1	1	-	PG
PG2	1	0.2	PG
PG3	1	1	PG
WP1	1	-	WP
WP2	1	0.2	WP
WP3	1	1	WP

138

139 The solutions were freshly prepared before the experiments. For PG2, PG3, WP2, and
 140 WP3, mixing of the ingredients was performed with mild stirring to avoid foam formation by
 141 CPC.

142

143 2.2.2. Skin PAMPA studies

144 *Influence of CPC on PAMPA membrane integrity*

145 In order to assess the compatibility of the skin PAMPA membrane with CPC, permeation
 146 of CPC in the PAMPA model was monitored over 6 h. For these tests, CPC was dissolved in
 147 PG at a final concentration of 0.2% w/w and 1% w/w. The permeation studies were performed
 148 using the same setup as described in the previous section. Eight different doses were used,
 149 covering finite and infinite conditions: 6, 10, 18, 30, 103, 515, 181, and 909 $\mu\text{g}/\text{cm}^2$. To achieve
 150 these doses, CPC was applied at application volumes of 1, 3, 17, and 30 μL .

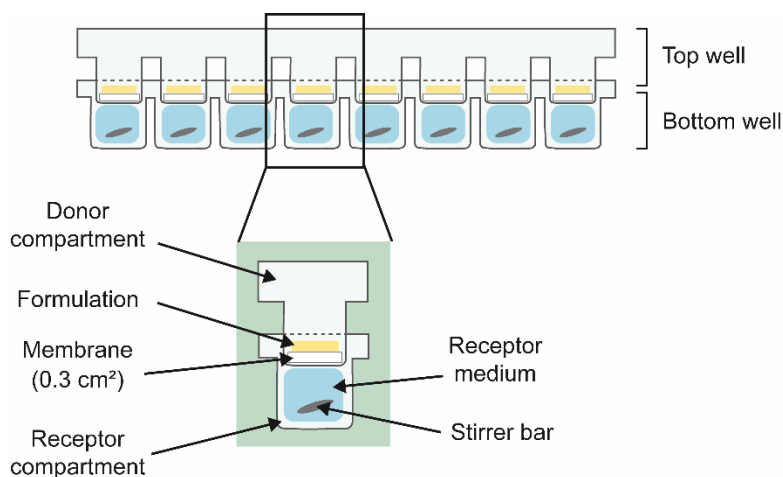
151

152 *Permeation of PE in the skin PAMPA membrane*

153 Permeability of PE was investigated in the skin PAMPA membrane using a modified
 154 procedure reported by Luo et al. and Zhang et al. (Luo et al., 2016; Zhang et al., 2019). The
 155 setup for this assay is illustrated in Fig. 1. The top side of the skin PAMPA sandwich plate was
 156 set as the donor compartment, where the test solution was applied. For pilot studies, the dose
 157 of PE applied was varied from 3 to 6-9 $\mu\text{L}/\text{cm}^2$ to assess the suitability of the experimental
 158 design. Based on the results, an applied dose of 6-9 $\mu\text{L}/\text{cm}^2$ was selected for the remaining
 159 experiments.

160 The collector plates were added with stirring disks and filled with 180 μl of degassed
161 PBS (pH 7.30 ± 0.10). Following application of the test solution, the two plates were assembled
162 and incubated in the Gut-Box™ stirring unit at 32 ± 1 °C for 1 h. The collector plate was
163 replaced with a new plate prefilled with receptor solution at 1, 2, 5, 10, 15, 20, 30, 45, and 60
164 min.

165



166

167 **Fig. 1.** Experimental setup for skin PAMPA studies.

168

169 2.2.3. Franz cell studies

170 Skin permeation studies

171 Permeation studies were conducted using full-thickness porcine skin and heat-
172 separated human epidermis in Franz-type diffusion cells. Porcine skin was prepared as
173 described by Cristofoli et al. (Cristofoli et al., 2022). The epidermis of human skin was isolated
174 by the heat separation technique as described by Oliveira et al. (Oliveira et al., 2012). The
175 receptor medium was similar to that of the skin PAMPA assay. The permeation study was
176 conducted for 24 h at 32 ± 1 °C. Temperature was controlled by using a water bath (Sub Aqua
177 26 Plus, Grant™, Fischer Scientific, UK). Prior to the experiments, the skin impedance was
178 measured to assess the skin barrier integrity, as described previously (Oliveira et al., 2012).
179 The skin was then allowed to equilibrate to reach 32 ± 1 °C. The temperature of the skin was
180 measured using a digital thermometer (TM-22 Digitron, RS Components, UK). 10 μL of the
181 test solution, representing a finite dose of 10 $\mu\text{L}/\text{cm}^2$ (corresponding to 100 μg PE per cm^2),
182 was applied evenly on the donor compartment. 100 μL of sample was withdrawn at 0, 0.5, 1,
183 2, 4, 6, 8, 10, 12, and 24 h. After sample collection, volume replacement was carried out by

184 adding 100 μ L of receptor solution (maintained at 32 ± 1 °C) to the receptor compartment. All
185 samples were analyzed for PE and CPC content using a validated HPLC method (section
186 2.2.4).

187

188 *Mass balance studies*

189 At the end of the permeation study, the receptor medium was immediately removed. Each
190 donor compartment was washed with 1 mL of methanol-water (85:15) mixture and the washing
191 solution was transferred to a 2 mL microcentrifuge tube. The cap of the tube was sealed with
192 Parafilm® to prevent evaporation. The washing procedure was performed 3 times. The Franz
193 diffusion cells were then disassembled, and each skin membrane was transferred to a 2 mL
194 microcentrifuge tube. 1 mL of methanol-water (85:15) was added to the microcentrifuge tube
195 and the cap of the tube was sealed with Parafilm® to prevent evaporation. Extraction of PE
196 and CPC was carried out by placing the tubes in a bench shaker (VWR International, USA) at
197 800 rpm for 12 h. All samples were centrifuged using an Eppendorf® microcentrifuge 5415R
198 (Eppendorf, UK) at 13,200 rpm for 20 min. Subsequently, the samples were analyzed for PE
199 and CPC content using a validated HPLC method. The percentage of the two ingredients
200 recovered from the washing solution, extraction solution, and the receptor solution was
201 determined.

202

203 *2.2.4. Quantification of PE and CPC*

204 The determination of PE and CPC content was performed using HPLC with a diode-array
205 detector (Agilent Technologies 1200 Series). Data acquisition was performed using
206 Chemstation software (Agilent Technologies, USA). A Kinetex® XB-C₁₈ column (250 x 4.60
207 mm, Phenomenex, UK) was used for the analysis. All the samples and standard solutions
208 were stored in amber HPLC vials during the assay. Optimized HPLC conditions were achieved
209 using a gradient elution system. The elution conditions are shown in Table 23. The flowrate,
210 injection volume, and column temperature were set as 1 ml/min, 20 μ L, and 40 °C,
211 respectively. The detection wavelengths were 258 nm (for CPC) and 270 nm (For PE).

212

213

214 **Table 23.** Elution conditions for PE and CPC.

Time	Volume ratio of mobile phase (%)	
	acetonitrile	0.1% TFA
	0 – 4	28
5 – 9 <u>12</u>	80	20
10 – 12	28	30
13 – 16	28	72

215

216 Validation of the analytical method was carried out in accordance with the guidelines
 217 outlined by the International Conference on Harmonization (ICH) regarding quantitative
 218 assays for determination of the content of active compounds (ICH Harmonised Tripartite,
 219 2005). The following parameters were assessed: linearity, range, accuracy, intra-day and
 220 inter-day precision, limit of detection (LOD), limit of quantification (LOQ), and robustness. In
 221 addition, a system suitability test was performed to ensure that consistent chromatographic
 222 behavior was achieved for each analytical procedure (US Food and Drug Administration,
 223 1994).

224

225 2.2.5. Statistical analysis

226 Statistical analysis was performed using Origin 8.0 (OriginLab Corp., Northampton, MA).
 227 Data were assessed for normal distribution and homogeneity using the Shapiro-Wilk Test and
 228 Levene's Test, respectively. Sets of data that met the assumptions of normality and
 229 homogeneity were analyzed using one-way ANOVA followed by Tukey's post hoc test. The
 230 Kruskal–Wallis H Test was used for datasets that did not follow the assumptions of normality
 231 and/or homogeneity of variance. The level of significance was set at a p-value lower than 0.05
 232 ($p < 0.05$). The correlation assessment was performed using the Pearson correlation coefficient
 233 (r^2).

234

235 3. Results

236 3.1. HPLC method validation

237 The results of method validation are shown in Table ~~34~~34. The retention times of PE and
 238 CPC using the validated method were 6.01 and 9.40 min, respectively. The linearity for PE
 239 and CPC was obtained for a concentration range of 1 to 100 $\mu\text{g/mL}$. The calibration curve
 240 from this range of concentrations exhibited a linear regression line. The LOD and LOQ for PE

241 were calculated as 0.49 µg/mL and 1.49 µg/mL, respectively. The LOD and LOQ for CPC
 242 were 0.51 µg/mL and 1.55 µg/mL, respectively.

243

244 **Table 34.** Summary of validation parameters for PE and CPC analysis using HPLC

Parameters	PE	CPC
Linearity range (µg/mL)	1 – 100	1 – 100
r ²	>0.99	>0.99
LOD (µg/mL)	0.49	0.51
LOQ (µg/mL)	1.49	1.55
Accuracy		
Recovery (%)	100.07 ± 0.34	100.42 ± 0.59
RSD (%)	0.03 – 0.65	0.04 – 0.89
Precision		
Intra-day (%RSD)	0.17	0.42
Inter-day (%RSD)	0.25	1.14
Robustness (r ²)	>0.99	>0.99
System suitability		
peak area (%RSD)	0.16	0.59
RT (%RSD)	0.10	0.10
Peak symmetry (%RSD)	0.99	0.18

245 RSD = relative standard deviation

246

247 The accuracy, which represents the closeness between the experimentally measured
 248 values and the true values, was determined by measuring the response of blank samples
 249 spiked with PE and CPC at 5, 50, and 100 µg/mL, representing the low, medium, and high
 250 concentrations. The average recovery value for PE was 100.07 ± 0.34 %, with a relative
 251 standard deviation (RSD) value <1%. As for CPC, the recovery value was 100.42 ± 0.59 %,
 252 with an RSD value <1.00%. The precision of the method was assessed based on intra-day
 253 and inter-day precision assessments. The RSD of the measured concentrations was used to
 254 express the inter-assay variability. Acceptable precision was achieved with corresponding
 255 RSD values of <1.00% and <2.00% for intra-day and inter-day assessment, respectively.

256 The robustness of an analytical method is investigated to ensure that the capability of
 257 the HPLC system remains unaffected with minor variations in chromatographic conditions.

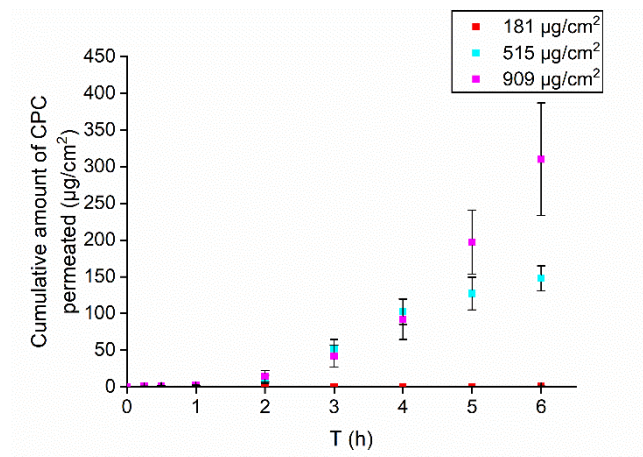
258 The robustness test was performed on standard solutions containing PE and CPC within a
259 concentration range of 1-100 $\mu\text{g}/\text{mL}$. Despite the minor variations (2% change) in injection
260 volume, flow rate, column temperature, mobile phase composition, and detection wavelength,
261 r^2 values remained ≥ 0.99 . A system suitability test was performed by determining the RSD of
262 the injection repeatability, as described in the Reviewer Guidance on Validation of
263 Chromatographic Methods (US Food and Drug Administration, 1994). Six injections of
264 solutions with PE and CPC at a concentration of 50 $\mu\text{g}/\text{mL}$ were determined for the peak area,
265 peak symmetry, and retention time. The RSD values for these parameters were $\leq 1.00\%$ for
266 PE and CPC.

267

268 3.2. Influence of CPC on PAMPA membrane integrity

269 Fig. 2 compares the amount of CPC permeated from different applied doses. When the
270 applied dose was $\leq 103 \mu\text{g}/\text{cm}^2$, permeation of CPC was not detected over 6 h. For the 181
271 $\mu\text{g}/\text{cm}^2$ dose, permeation of CPC was evident from 5 h. The amount of CPC permeated for
272 this dose was $0.06 \pm 0.07 \mu\text{g}/\text{cm}^2$ at 5 h. At the higher dose of CPC ($\geq 515 \mu\text{g}/\text{cm}^2$), the
273 permeation of CPC was observed at earlier timepoints.

274



275

276 **Fig. 2.** The amount of CPC permeated through the skin PAMPA membrane under various
277 applied doses (mean \pm SD, n = 6).

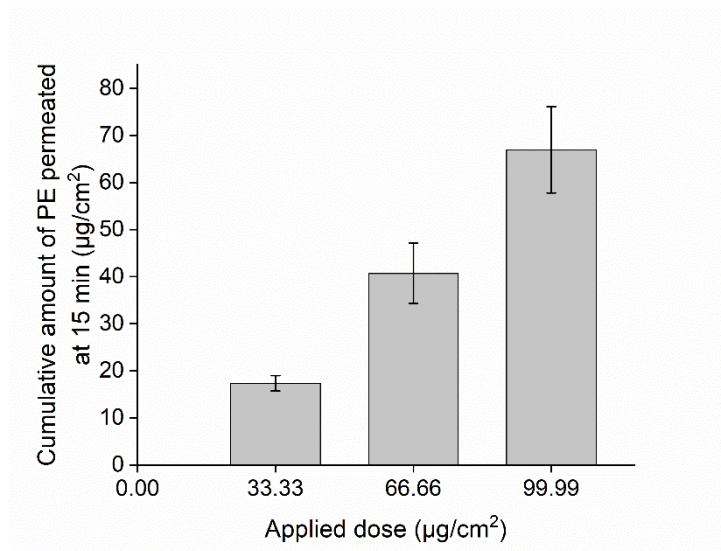
278

279

280 3.3. Permeation of PE in the skin PAMPA membrane

281 Cumulative amounts of PE permeated through the skin PAMPA membrane from different
 282 applied doses are shown in Fig. 3. Three PE doses were used in this set of experiments – 1,
 283 2, and 3 μL . These doses corresponded to 3, 6, and 9 $\mu\text{L}/\text{cm}^2$.

284



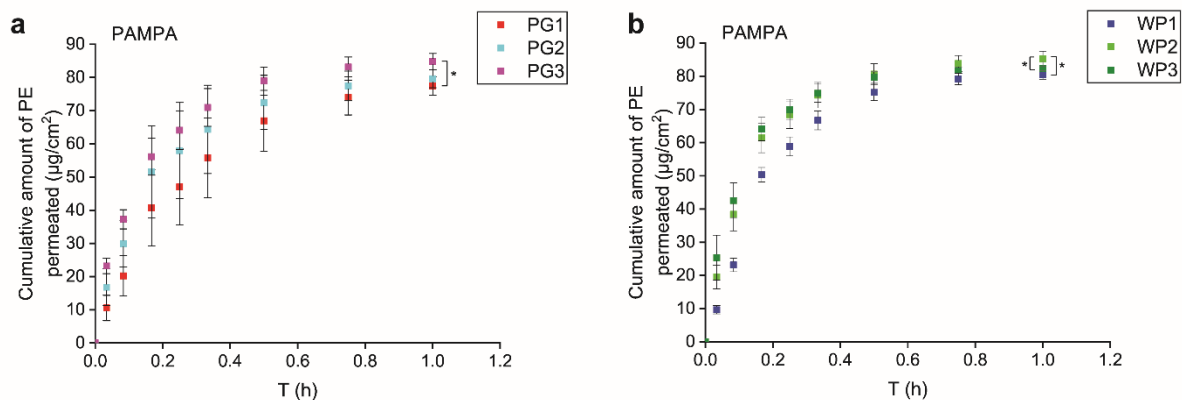
285

286 **Fig. 3.** Cumulative amounts of PE permeated through the skin PAMPA membrane from the
 287 different applied doses (mean \pm SD, n = 6).

288

289 The permeation profiles of PE in the skin PAMPA model are shown in Fig. 4.
 290 Permeation of PE was evident from 1 min. The highest permeation of PE was observed for
 291 the solution containing CPC 0.2% with water-PG as the vehicle. The cumulative amount of PE
 292 that permeated from this preparation was $85.30 \pm 2.19 \mu\text{g}/\text{cm}^2$. For preparations with neat PG
 293 as the solvent, a significantly higher amount ($p < 0.05$) of PE permeated from the vehicle with
 294 CPC 1%, compared with the PE solution with no CPC.

295



296

297 **Fig. 4.** Permeation profiles of PE from (a) PG and (b) Water-PG in the skin PAMPA
298 membrane (mean \pm SD, n = 6). * ~~indicates~~Indicates statistical significance ($p < 0.05$)
299 compared to the ~~rest of other~~ preparations.
300

301 Interestingly, for water-PG preparations, the cumulative amount of PE permeated was
302 significantly higher ($p < 0.05$) in the presence of CPC 0.2% compared with all other PE
303 solutions. These findings suggested that the increase in PE permeation from water-PG was
304 not necessarily proportional to the concentration of CPC.

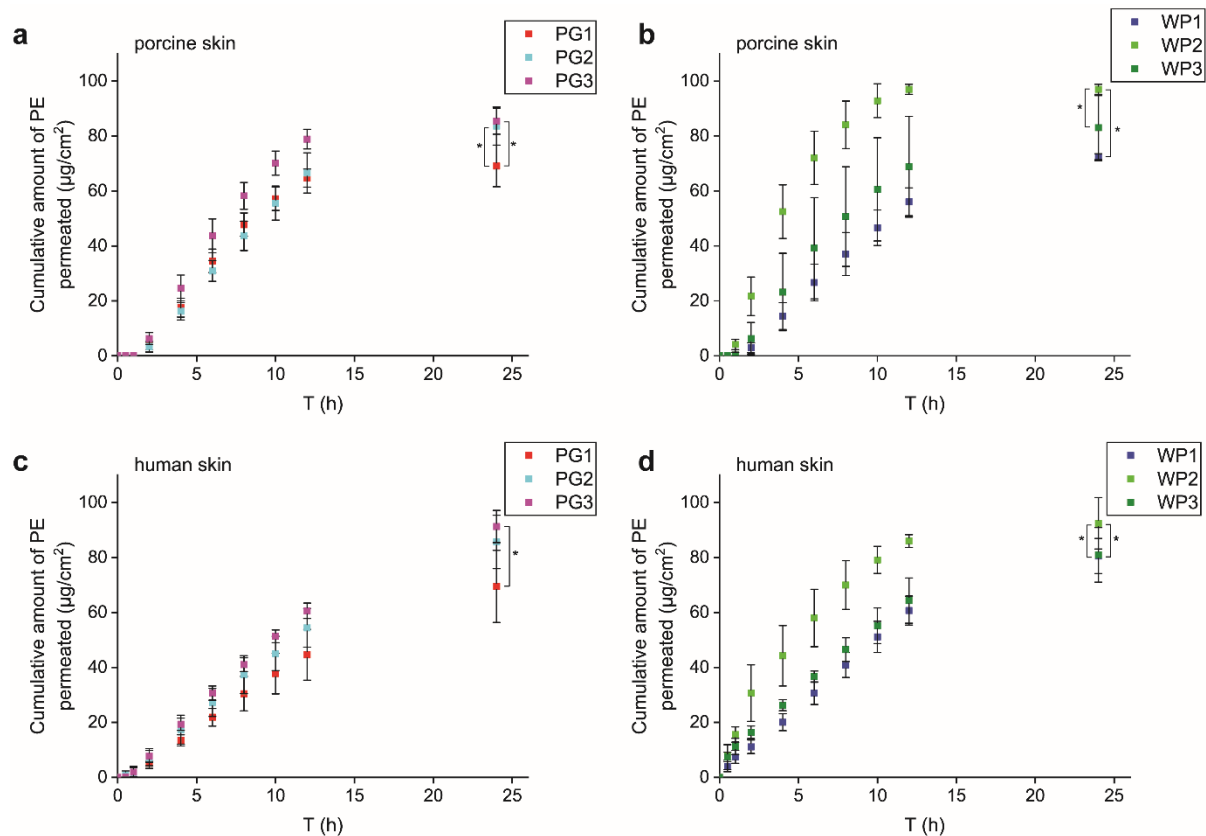
305

306 3.4. Franz cell studies

307 3.4.1. Permeation of PE in porcine skin and human skin

308 The permeation profiles of PE in porcine skin and human skin are shown in Fig. 5. We
309 observed a trend which was consistent with the skin PAMPA data, where the highest
310 permeation of PE was observed for water-PG with 0.2% of CPC. The cumulative amounts of
311 PE that permeated in porcine skin and human skin from this preparation at 24 h were $96.98 \pm$
312 $1.83 \mu\text{g}/\text{cm}^2$ and $92.46 \pm 9.34 \mu\text{g}/\text{cm}^2$, respectively. These values corresponded to more than
313 97% of the applied dose. The lowest permeation of PE was observed for PG without CPC,
314 both in porcine skin and human skin ($69.09 \pm 7.54 \mu\text{g}/\text{cm}^2$ and $73.99 \pm 9.70 \mu\text{g}/\text{cm}^2$,
315 respectively). These results are consistent with the skin PAMPA data.

316



317

318 **Fig. 5.** Permeation profiles of PE from various preparations in porcine skin and human skin.
 319 (a) PG vehicle applied to porcine skin; (b) Water-PG vehicle applied to porcine skin; (c) PG
 320 vehicle applied to human skin; (d) Water-PG vehicle applied to human skin. Mean \pm SD, n =
 321 5-6. * indicates statistical significance ($p < 0.05$) compared to the rest of other
 322 preparations.

323

324 Regarding the effect of CPC on the permeation of PE, the results from porcine skin and
 325 human skin studies were consistent with the trends observed in the skin PAMPA studies. For
 326 PG, a significantly higher cumulative amount of PE permeation was evident in the presence
 327 of CPC 1% compared to preparations with no CPC ($p < 0.05$). This was observed both in
 328 porcine skin and human skin. For water-PG, the cumulative amount of PE permeated was
 329 significantly higher ($p < 0.05$) in the presence of CPC 0.2% compared with all other PE vehicles.

330

331 3.4.2. Mass balance studies for PE and CPC in porcine skin and human skin

332 The results of the mass balance studies for PE are shown in Table 45. The amount of PE
 333 that remained on the surface of porcine skin was 1-2% a maximum of 2.01% of the applied
 334 dose for the PG vehicle. In contrast, PE was not detected in the washing solution for all water-

335 PG preparations. For human skin data, the amount of PE that remained on the skin surface
 336 for the PG vehicle was ~~up to a maximum of~~ 27.08% of the applied dose. Similar to the findings
 337 from porcine skin, PE was not detected in the washing solution for all water-PG preparations.
 338 Regarding the skin retention of PE, the percentages of the active recovered from the porcine
 339 skin for PG vehicle were ~~around~~ 8.19-9.37% of the applied dose. For the water-PG
 340 preparations, ~~around~~ 8.61-13.25% of PE was retained in porcine skin. The percentages of PE
 341 retained in human skin were lower than in porcine skin. At the end of the permeation studies,
 342 3.08–3.57% of PE from the PG preparations were recovered in human skin. For the water-PG
 343 preparations, the percentage of PE extracted from human skin was 1.10–1.27%.

344

345 **Table 45.** Mass balance results for PE in porcine skin and human skin (mean ± SD, n = 5).

Preparation	PE recovered (% of applied dose)			
	Receptor fluid	Skin surface	Skin	Total recovery
Porcine skin				
PG1	81.32 ± 6.03	1.47 ± 1.09	9.20 ± 2.44	92.00 ± 4.97
PG2	85.23 ± 5.22	2.01 ± 0.57	9.37 ± 0.98	96.61 ± 4.96
PG3	92.51 ± 3.39	ND	8.19 ± 0.82	100.70 ± 2.83
WP1	79.00 ± 4.04	ND	13.25 ± 2.99	92.25 ± 1.77
WP2	95.81 ± 9.45	ND	8.61 ± 0.94	104.49 ± 8.56
WP3	88.29 ± 10.28	ND	10.06 ± 2.86	98.36 ± 13.14
Human skin				
PG1	71.40 ± 12.62	27.08 ± 8.17	3.57 ± 0.12	102.06 ± 4.65
PG2	83.63 ± 2.48	11.17 ± 3.09	3.41 ± 0.28	98.23 ± 0.64
PG3	97.34 ± 3.59	4.24 ± 3.82	3.08 ± 0.55	104.67 ± 0.73
WP1	89.07 ± 2.75	ND	1.11 ± 0.17	90.19 ± 2.92
WP2	97.79 ± 6.66	ND	1.10 ± 0.16	98.89 ± 6.68
WP3	87.90 ± 7.05	ND	1.27 ± 0.12	89.18 ± 7.02

346 ND = not detected

347

348 In contrast to PE, permeation of CPC was not detected in porcine skin and human skin
 349 studies for all preparations, as was observed in the skin PAMPA model. Mass balance results
 350 using porcine skin (Table 56) showed that the amount of CPC that remained on the skin
 351 surface varied between 61.31 to 95.28% of the applied dose, whereas the amount of CPC
 352 retained in the skin was 10.28-38.72% of the applied dose. In contrast, mass balance studies

353 using human skin confirmed that more than 80% of the applied dose of CPC was recovered
 354 from the skin surface for all vehicles (Table 56).
 355

356 **Table 56.** Mass balance results for CPC in porcine skin and human skin (mean \pm SD, n = 5).

Preparation	Receptor fluid	CPC recovered (% of applied dose)		
		Skin surface	Skin	Total recovery
Porcine skin				
PG2	ND	83.21 \pm 8.44	21.12 \pm 7.68	104.33 \pm 1.19
PG3	ND	95.28 \pm 4.29	10.28 \pm 4.45	105.57 \pm 0.16
WP2	ND	61.31 \pm 0.87	38.72 \pm 1.99	100.04 \pm 2.16
WP3	ND	82.71 \pm 3.25	13.00 \pm 2.52	95.71 \pm 2.28
Human skin				
PG2	ND	85.06 \pm 8.07	8.81 \pm 1.13	93.88 \pm 7.01
PG3	ND	91.40 \pm 14.03	3.33 \pm 3.00	94.74 \pm 11.48
WP2	ND	90.04 \pm 9.87	7.72 \pm 2.33	97.77 \pm 7.84
WP3	ND	89.92 \pm 7.25	1.71 \pm 91.64	91.64 \pm 8.13

357 ND = not detected

358

359 **3.5. Comparative evaluation of the permeation data**

360 Cumulative amounts of PE that permeated the skin PAMPA membranes, porcine skin, and
 361 human skin are shown in Fig. 6. Statistical differences in the amount of PE that permeated
 362 from various preparations were assessed within the same vehicles rather than all vehicles.
 363 This approach should provide a clearer insight into possible active-vehicle-membrane
 364 interactions.

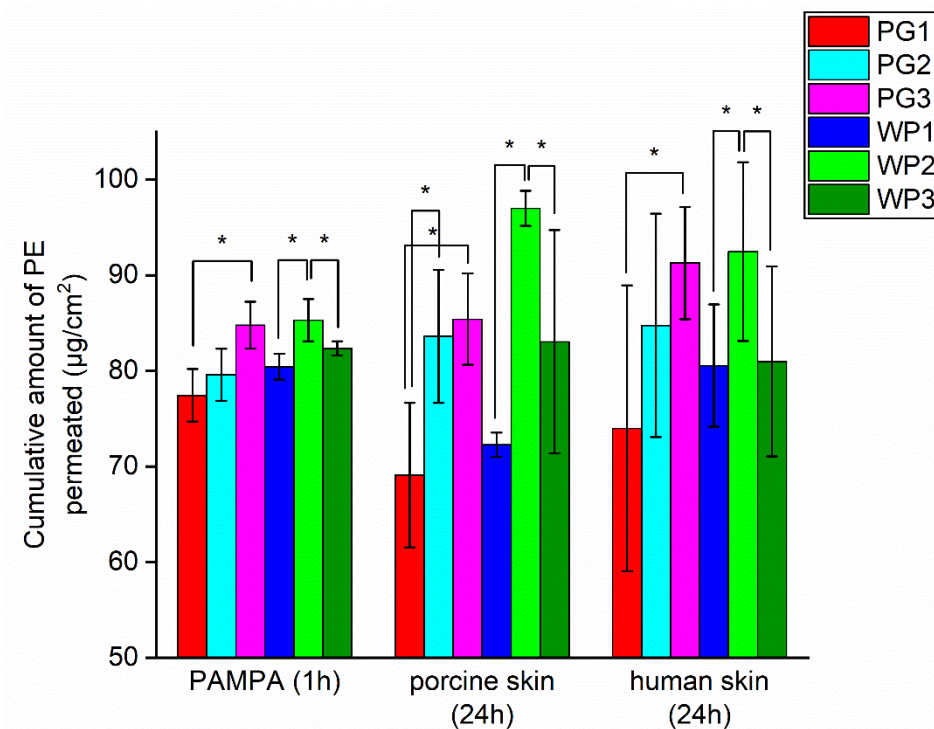
365

366

367

368

369



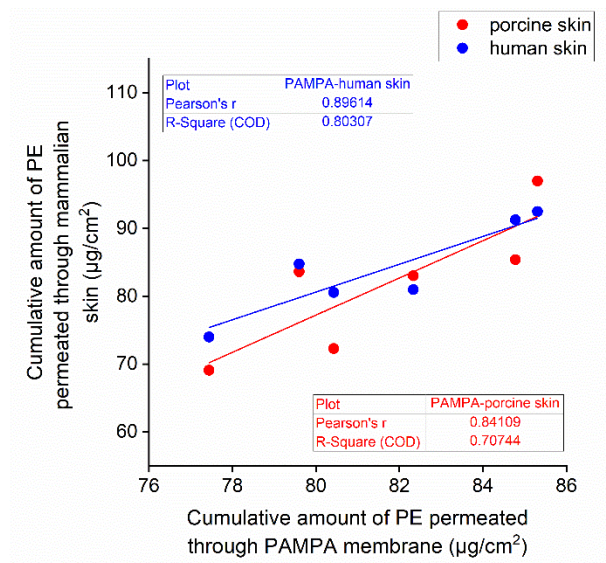
370

371 **Fig. 6.** Cumulative amounts of PE that permeated the membranes (mean ± SD, n = 5-6).

372 * indicates statistical significance (p<0.05) compared to the rest of other preparations within
 373 the same vehicle and within the same membrane model.

374

375 Correlations for the cumulative amount of PE permeated between the skin PAMPA data
 376 and the mammalian skin data are shown in Fig. 7. When comparing the skin PAMPA data and
 377 the porcine skin data for cumulative amount of PE permeated, the r^2 value was 0.84. This
 378 value is consistent with previously reported data by Zhang et al. (Zhang et al., 2019). For the
 379 correlation between the skin PAMPA and human skin data for cumulative amount of PE
 380 permeated the corresponding r^2 value was 0.89.



381

382

383

384

Fig. 7. Correlation between cumulative amounts of PE that permeated through skin PAMPA and mammalian skin. Each point represents the mean value (n = 5-6).

385

4. Discussion

386

387

388

389

390

391

392

393

394

395

396

397

398

399

400

401

402

403

404

Synthetic membranes mimicking the stratum corneum (SC) have been investigated extensively as surrogate models for *in vitro* skin permeation studies (Čuříková et al., 2017; de Jager et al., 2006b; Groen et al., 2011; Sinkó et al., 2012; Uchida et al., 2015). The membranes are composed of a porous substrate coated with synthetic SC lipids, which serve as the rate-determining barrier for skin permeation. In the present work, preliminary assessment of skin PAMPA compatibility with CPC was conducted prior to permeation studies for CPC-containing preparations. It is important to evaluate the compatibility of synthetic membranes with formulations, particularly when the formulation contains penetration enhancers (Köllmer et al., 2019; Kovács et al., 2021). Surfactants have been reported to have the potential to disrupt the organization of the SC lipids, although the mechanism underlying this is not fully understood (Gloor et al., 2004; Jiang et al., 2003). The interaction between surfactants and SC lipids is complex, depending on the duration of exposure, the nature, and the concentration of the surfactants (De la Maza et al., 1997; Imokawa, 2004; Rhein et al., 1986). Köllmer et al. recently investigated the compatibility of the skin PAMPA membrane with different surfactants (Köllmer et al., 2019). In their study, the skin PAMPA membrane was incubated with blank formulations which contained different surfactants (1% Brij™ S2 + 0.15% Brij™ S721 and 1% Brij™ S2 + 1% Brij™ S721). After 4 h of pre-incubation, a permeation test was performed for methylparaben, ethylparaben, and propylparaben for 4 h. The results indicated that pre-incubation with these surfactants did not increase the permeation of the parabens. In addition,

405 the rank order for permeation remained unchanged (methylparaben > ethylparaben >
406 propylparaben). The authors suggested that the surfactants used in the study did not alter the
407 permeability of the skin PAMPA membrane towards the parabens (Köllmer et al., 2019).

408 In the present study, permeation of CPC was not detected over 6 h when the application
409 dose was $\leq 103 \mu\text{g}/\text{cm}^2$. The concentration of CPC used in the permeation studies for PE-
410 containing vehicles using the skin PAMPA model was not more than $30 \mu\text{g}/\text{cm}^2$. In addition,
411 the duration of the experiment was only 1 h. Permeation of CPC from all vehicles was not
412 detected in the receptor solution over 1 h. More importantly, a comparison with the Franz cell
413 studies confirmed that the permeation data from the skin PAMPA model showed a good
414 correlation with the porcine skin and human skin data (Fig. 7). Therefore, no evident
415 incompatibility was observed between the skin PAMPA membrane with the vehicles used in
416 this study under previously mentioned conditions.

417 Possible membrane-excipient interactions such as membrane blockage by the
418 formulation, disorganization or solubilization of the membrane lipids have also been
419 recognized (Köllmer et al., 2019). Two recent studies reported the effects of several excipients
420 on the permeation of actives in the skin PAMPA membrane (Kovács et al., 2021; Zhang et al.,
421 2019). Zhang et al. reported that niacinamide permeated the skin PAMPA membrane from
422 PEG 400 and PEG 600, whereas it did not permeate in porcine and human skin studies (Zhang
423 et al., 2019). These authors suggested that this might reflect the interaction between those
424 solvents and the skin PAMPA membrane.

425 Finite dose experiments using the skin PAMPA model reported by Luo et al. and Zhang et
426 al. included application doses as low as $3 \mu\text{L}/\text{cm}^2$ (Luo et al., 2016; Zhang et al., 2019). These
427 studies reported comparable results for permeation profiles. ~~The latter study reported a good~~
428 ~~correlation for cumulative amount~~ of the actives (ibuprofen, niacinamide) between the skin
429 PAMPA model and porcine skin as well as human skin. In the current study, permeation of PE
430 at the $3 \mu\text{L}/\text{cm}^2$ dose in the skin PAMPA membrane had reached a plateau at 45 min. As
431 frequent sampling within such a short period was impractical and permeation data showed
432 high variability, a dose of $9 \mu\text{L}/\text{cm}^2$ was selected as the final dose for PE. As shown in Fig. 3,
433 it is evident that by using the skin PAMPA model, a 1 h study time was sufficient for PE to
434 demonstrate comparable finite dose kinetics to those observed in porcine skin and human skin
435 in 24 h. Even with relatively high permeation of PE over a short period, the skin PAMPA model
436 was also capable of discriminating between different preparations. This was reflected by the
437 statistical differences between the formulations for the cumulative amounts of PE permeated,
438 as was observed in the porcine skin and human skin studies (Fig. 6). Such high-throughput
439 prediction in a time efficient manner is expected to be particularly useful for screening

440 numerous topical formulations (Luo et al., 2016; Neupane et al., 2020; Sinkó et al., 2012;
441 Zhang et al., 2019). Consistent with previously reported studies, the time required for the
442 active to permeate the artificial membrane was shorter compared with porcine skin or human
443 skin (Čuříková et al., 2017; Kovács et al., 2021; Luo et al., 2016; Zhang et al., 2019). In
444 addition, the variability in the skin PAMPA data, represented by the standard deviation, was
445 lower than in the Franz cell studies with mammalian tissue.

446 As shown in Fig. 4, the highest permeation of PE in the skin PAMPA model was observed
447 for water-PG with 0.2% of CPC. This finding was consistent with observations in the Franz cell
448 studies using porcine skin and human skin (Fig. 5). This concentration of CPC is typically used
449 in commercial baby wipe formulations, which comprise more than 90% of water and a low
450 concentration of surfactant (< 0.5%). On the other hand, the three permeation models
451 confirmed that the lowest permeation of PE was observed for neat PG without CPC. These
452 results also correspond with the findings from a study by Luo et al., where the highest amount
453 of active (ibuprofen) that permeated the skin PAMPA model was observed for the formulation
454 which delivered the highest amount of active in human skin under finite dose conditions (Luo
455 et al., 2016).

456 While permeation of CPC was not detected in the skin PAMPA model and Franz cell
457 studies, the presence of CPC enhanced the permeation of PE significantly ($p < 0.05$) compared
458 with preparations without CPC. Interestingly, better enhancement for permeation of PE was
459 observed when the CPC concentration was 1% for PG and 0.2% for water-PG. The results of
460 permeation studies using human skin showed that the cumulative amounts of PE permeated
461 from PG in the presence of CPC 0.2% and 1% were 14% and 23% higher, respectively,
462 compared with PE alone. For water-PG, the presence of CPC at 0.2% and 1% resulted in
463 enhanced PE permeation by 14% and 0.5%, respectively, compared to PE alone. This might
464 indicate that CPC influences the permeation of PE from PG and water-PG by different
465 mechanisms. In general, it has been thought that the alkyl chains of surfactants may
466 intercalate with the hydrophobic regions of the SC lipids (Gloor et al., 2004; Jiang et al., 2003).
467 The ability of surfactants to increase the permeation of various actives is well documented
468 (Merwe and Riviere, 2005; Riviere et al., 2010; Shokri et al., 2001). Clearly, it should be noted
469 that surfactants are able to form micelles, enhance the solubility of permeant and thus reduce
470 its thermodynamic activity (Lane, 2013). The critical micellar concentration of CPC was
471 reportedly 1 mM (approximately 0.34 mg/mL) in water at 25 °C (Wang et al., 1999). In the
472 present work, the concentrations of CPC used were 2 mg/mL and 10 mg/mL. For WP, the
473 vehicle with 97% water, CPC was present above the CMC which may explain the results
474 observed.

475 Regarding the correlation between the skin PAMPA data and mammalian skin data, the r^2
476 values for skin PAMPA-porcine skin and skin PAMPA-human skin were 0.84 and 0.89,
477 respectively (Fig. 7). Previously, Zhang et al. reported that the correlation for the permeation
478 of niacinamide between the skin PAMPA studies and porcine skin studies was 0.88 under
479 finite dose conditions. However, the corresponding r^2 value for human skin was lower
480 compared to porcine skin, namely 0.71.

481 It is important to note that artificial membranes are not intended to provide an estimation
482 of the amount of actives that permeate the human skin since these membranes do not fully
483 represent the biological complexity of human skin (Čuříková et al., 2017; Neupane et al.,
484 2020). Such models can be used as an initial screening tool before performing permeation
485 studies using human skin (Neupane et al., 2020; Zhang et al., 2019). Recently, a
486 comprehensive overview of the findings from permeation studies using synthetic membranes
487 was reported by Neupane et al. (Neupane et al., 2020). The main advantages of artificial
488 membranes are less variability in the thickness and composition compared with biological
489 tissues, and ease in storage (Neupane et al., 2020). A number of studies have demonstrated
490 the ability of artificial membranes to correlate with *ex vivo* permeation studies using porcine
491 skin or human skin (Balázs et al., 2016; Čuříková et al., 2017; de Jager et al., 2006a; Groen
492 et al., 2011; Sinkó et al., 2021; Sinkó et al., 2012; Uchida et al., 2015). However, most of the
493 studies were conducted under infinite dose conditions. On the other hand, finite dose
494 experiments are more relevant for prediction of dermal absorption with reference to the
495 amount of formulation applied in the real clinical setting. In finite dose experiments, the
496 implications of evaporation and residence time of the solvents, as well as the solubility of the
497 active in the remaining formulation should be taken into consideration (Lane, 2013).
498 Correlations observed in comparative studies using infinite dose conditions should not be
499 directly assumed to hold true for finite dose situations. As mentioned earlier, Zhang and co-
500 workers reported that the skin PAMPA data showed correlations with the porcine skin and
501 human skin data, for the amount of active permeated, under finite dose conditions but not
502 under infinite dose conditions (Zhang et al., 2019).

503 The importance of lipid composition for permeability of artificial membrane models has
504 been studied extensively. Groen et al. described the importance of lipid compositions
505 (cholesterol free fatty acid, and ceramide) for the permeability of skin lipid models (Groen et
506 al., 2011). In this study, the authors investigated the permeability of a stratum corneum
507 substitute (SCS) with various ratios of SC lipids. This was done by assessing the permeation
508 of benzoic acid under infinite dose conditions. It was found that the permeability of SCS to
509 benzoic acid was higher when the SCS membrane contained a high content of free fatty acids.
510 In contrast, permeation of benzoic acid was lower for SCS with high cholesterol or ceramide

511 content compared to SCS with equimolar composition of cholesterol free fatty acid, and
512 ceramide.

513 A synthetic ceramide named certramide is used in the skin PAMPA membrane (Sinkó et
514 al., 2012). Certramides are long-chain tartaric acid diamide derivatives. In the skin PAMPA
515 membrane, the length of the alkyl chains in the certramides are 8 and 18 (C8-C18). The
516 ceramides was are used as ceramide analogs with long alkyl chains combined with stearic acid
517 and cholesterol (Sinkó et al., 2012). The ratio of the membrane components in the skin
518 PAMPA model (~~certramides, stearic acid and cholesterol~~) was chosen to represent the
519 intercellular lipid matrix of the SC (Sinkó et al., 2012). The membrane, which demonstrated
520 positive correlation with human SC for permeation of various compounds (Sinkó et al., 2012).
521 The effects of molecular structure of ceramides on the permeability of a SC lipid model
522 membrane ~~has~~ have previously been reported (Čuříková et al., 2017; Školová et al., 2013).
523 Školová and co-workers reported a decrease in permeability of the studied synthetic
524 membrane ~~towards for~~ two drugs models (theophylline and indomethacin) when natural long-
525 chain ceramides (24-acyl chains, Cer24) ~~was~~ were incorporated into the membrane
526 compared to a control model without Cer24. Increased permeation for both model compounds
527 was observed when short-chain ceramides (4-6 acyl chains) were used rather than the long-
528 chain ceramides. Čuříková et al. investigated the potential of simplified SC membranes to
529 predict the effects of permeation enhancers on the permeation of actives (Čuříková et al.,
530 2017). This membrane model is composed of stearic acid, cholesterol, cholesterol sulfate, and
531 ceramides. The ceramides used in the study ~~was~~ were simplified, consisting of N-2-
532 hydroxystearoyl phytosphingosine (CER[AP]) and/or N-stearoyl phytosphingosine (CER[NP]),
533 rather than more complex ceramides mixtures as developed earlier by de Jager et al. (de
534 Jager et al., 2006b). ~~In the study, the~~ The optimized membrane, containing an equimolar
535 mixture of CER[AP] and CER[NP], was used to examine the permeation of two active models,
536 indomethacin and theophylline from formulations with different permeation enhancers. For
537 both actives, the enhancement of permeation by N-dodecyl azepan-2-one (Azone) and (S)-N-
538 acetylproline dodecyl ester (L-Pro2) observed in the membrane model was consistent with ~~the~~
539 porcine skin studies conducted under infinite dose conditions.

540

541 **5. Conclusions**

542 This work confirms the potential of the PAMPA model as ~~an~~ important tool to discriminate
543 between different vehicles for permeation of actives. In addition, a positive correlation between
544 the skin PAMPA model and the Franz cell studies using porcine skin and human skin was
545 observed for the cumulative amount of PE permeated. Both the skin PAMPA model and Franz

546 cell studies using mammalian skin showed that the highest permeation of PE was observed
547 for CPC 0.2% in water-PG, which is the typical amount of CPC used in commercial baby wipe
548 formulations. Considering that skin cleansing using baby wipes is carried out regularly, the
549 findings of the current study may have implications for the safety evaluation of such products.
550 The three permeation models showed that the presence of CPC enhanced the permeation of
551 PE significantly ($p < 0.05$) compared with preparations without CPC. A greater enhancement
552 for permeation of PE was observed when [the](#) CPC concentration was 1% for PG and 0.2% for
553 water-PG. No evident incompatibilities between the skin PAMPA membrane and the examined
554 preparations were observed. Based on the present study and previous PAMPA publications it
555 is worth noting that the optimum experimental conditions for this model may vary for different
556 compounds. Future work will expand the range of actives to be studied in the model and further
557 investigate the application of the PAMPA model in high-throughput screening studies for
558 development of dermal formulations.

559

560

561 **Acknowledgement**

562 We thank our colleagues from the UCL Skin Research Group who provided insight and
563 expertise that greatly assisted the research. A.R. is grateful for financial support from The
564 Ministry of Finance of The Republic of Indonesia (Grant Ref: S-1778/LPDP.4/2019).

565

566 **Conflict of Interest**

567 The authors declare no conflict of interest.

568

569 **References**

- 570 Balázs, B., Vizserálek, G., Berkó, S., Budai-Szűcs, M., Kelemen, A., Sinkó, B., Takács-Novák, K., Szabó-
571 Révész, P., Csányi, E., 2016. Investigation of the Efficacy of Transdermal Penetration Enhancers
572 Through the Use of Human Skin and a Skin Mimic Artificial Membrane. *J. Pharm. Sci.* 105, 1134-1140.
- 573 Barbero, A.M., Frasch, H.F., 2009. Pig and guinea pig skin as surrogates for human in vitro
574 penetration studies: A quantitative review. *Toxicol. In Vitro* 23, 1-13.
- 575 Cristofoli, M., Hadgraft, J., Lane, M.E., Sil, B.C., 2022. A preliminary investigation into the use of
576 amino acids as potential ion pairs for diclofenac transdermal delivery. *Int. J. Pharm.* 623, 121906.
- 577 Cunningham, C., Mundschau, S., Seidling, J., Wenzel, S., 2008. Baby care, in: Schlossman, M. (Ed.),
578 The chemistry and manufacture of cosmetics, 2 ed. Allured, Chicago, pp. 1063-1154.
- 579 Cunningham, C.T., Seidling, J.R., Kroll, L.M., Mundschau, S.A., 2016. Stable emulsion for prevention
580 of skin irritation and articles using same. Google Patents.
- 581 Čuříková, B.A., Procházková, K., Filková, B., Diblíková, P., Svoboda, J., Kováčik, A., Vávrová, K.,
582 Zbytovská, J., 2017. Simplified stratum corneum model membranes for studying the effects of
583 permeation enhancers. *Int. J. Pharm.* 534, 287-296.
- 584 de Jager, M., Groenink, W., Bielsa i Guivernau, R., Andersson, E., Angelova, N., Ponec, M., Bouwstra,
585 J., 2006a. A Novel in Vitro Percutaneous Penetration Model: Evaluation of Barrier Properties with P-
586 Aminobenzoic Acid and Two of Its Derivatives. *Pharm. Res.* 23, 951-960.
- 587 de Jager, M., Groenink, W., van der Spek, J., Janmaat, C., Gooris, G., Ponec, M., Bouwstra, J., 2006b.
588 Preparation and characterization of a stratum corneum substitute for in vitro percutaneous
589 penetration studies. *Biochimica et Biophysica Acta (BBA) - Biomembranes* 1758, 636-644.
- 590 De la Maza, A., Coderch, L., Lopez, O., Baucells, J., Parra, J., 1997. Permeability changes caused by
591 surfactants in liposomes that model the stratum corneum lipid composition. *J. Am. Oil Chem. Soc.*
592 74, 1-8.
- 593 Dick, I.P., Scott, R.C., 1992. Pig Ear Skin as an In-vitro Model for Human Skin Permeability. *J. Pharm.*
594 *Pharmacol.* 44, 640-645.
- 595 Dreno, B., Zuberbier, T., Gelmetti, C., Gontijo, G., Marinovich, M., 2019. Safety review of
596 phenoxyethanol when used as a preservative in cosmetics. *J. Eur. Acad. Dermatol. Venereol.* 33, 15-
597 24.
- 598 Endo, Y., Mune, M., Usukura, J.U.N., 2020. Factors Affecting Reduction in Preservative Efficacy in
599 Nonwoven Fabrics. *Biocontrol Science* 25, 149-157.
- 600 European Union Scientific Committee on Consumer Safety, 2016. Opinion on Phenoxyethanol, in:
601 European Commission Health and Food Safety Directorate C: Public Health (Ed.).
- 602 Franz, T.J., 1975. Percutaneous absorption. On the relevance of in vitro data. *J. Invest. Dermatol.* 64,
603 190-195.
- 604 Franz, T.J., 1983. Kinetics of Cutaneous Drug Penetration. *Int. J. Dermatol.* 22, 499-505.

605 French National Agency for the Safety of Medicines and Health Products, 2019. Concentration of
606 phenoxyethanol in cosmetic products – Information statement.

607 Gloor, M., Wasik, B., Gehring, W., Grieshaber, R., Kleesz, P., Fluhr, J.W., 2004. Cleansing,
608 dehydrating, barrier-damaging and irritating hyperaemising effect of four detergent brands:
609 comparative studies using standardised washing models. *Skin Res. Technol.* 10, 1-9.

610 Groen, D., Poole, D.S., Gooris, G.S., Bouwstra, J.A., 2011. Investigating the barrier function of skin
611 lipid models with varying compositions. *Eur. J. Pharm. Biopharm.* 79, 334-342.

612 Hopf, N.B., Champmartin, C., Schenk, L., Berthet, A., Chedik, L., Du Plessis, J.L., Franken, A., Fräsch,
613 F., Gaskin, S., Johanson, G., Julander, A., Kasting, G., Kilo, S., Larese Filon, F., Marquet, F., Midander,
614 K., Reale, E., Bunge, A.L., 2020. Reflections on the OECD guidelines for in vitro skin absorption
615 studies. *Regul. Toxicol. Pharmacol.* 117, 104752.

616 Ibrahim, S.A., Li, S.K., 2009. Effects of chemical enhancers on human epidermal membrane:
617 Structure-enhancement relationship based on maximum enhancement (E(max)). *J. Pharm. Sci.* 98,
618 926-944.

619 Ibrahim, S.A., Li, S.K., 2010. Chemical enhancer solubility in human stratum corneum lipids and
620 enhancer mechanism of action on stratum corneum lipid domain. *Int. J. Pharm.* 383, 89-98.

621 ICH Harmonised Tripartite, 2005. Validation of analytical procedures: text and methodology Q2 (R1),
622 International Conference on Harmonization, Geneva, Switzerland.

623 Imokawa, G., 2004. Surfactant-induced depletion of ceramides and other intercellular lipids:
624 implication for the mechanism leading to dehydration of the stratum corneum. *Exogenous*
625 *Dermatology* 3, 81-98.

626 Jiang, S.J., Zhou, X.J., Sun, G.Q., Zhang, Y., Jiang, S.J., Sun, G.Q., Zhang, Y., 2003. Morphological
627 alterations of the stratum corneum lipids induced by sodium lauryl sulfate treatment in hairless
628 mice. *J. Dermatol. Sci.* 32, 243-246.

629 Kim, T.H., Kim, M.G., Kim, M.G., Shin, B.S., Kim, K.-B., Lee, J.B., Paik, S.H., Yoo, S.D., 2015.
630 Simultaneous determination of phenoxyethanol and its major metabolite, phenoxyacetic acid, in rat
631 biological matrices by LC–MS/MS with polarity switching: Application to ADME studies. *Talanta* 144,
632 29-38.

633 Köllmer, M., Mossahebi, P., Sacharow, E., Gorissen, S., Gräfe, N., Evers, D., Herbig, M.E., 2019.
634 Investigation of the Compatibility of the Skin PAMPA Model with Topical Formulation and Acceptor
635 Media Additives Using Different Assay Setups. *AAPS PharmSciTech* 20.

636 Kovács, A., Zsikó, S., Falusi, F., Csányi, E., Budai-Szűcs, M., Csóka, I., Berkó, S., 2021. Comparison of
637 synthetic membranes to heat-separated human epidermis in skin permeation studies in vitro.
638 *Pharmaceutics* 13.

639 Lane, M.E., 2013. Skin penetration enhancers. *Int. J. Pharm.* 447, 12-21.

640 Lehman, P.A., 2014. A Simplified Approach for Estimating Skin Permeation Parameters from In Vitro
641 Finite Dose Absorption Studies. *J. Pharm. Sci.* 103, 4048-4057.

642 Luo, L., Patel, A., Sinko, B., Bell, M., Wibawa, J., Hadgraft, J., Lane, M.E., 2016. A comparative study of
643 the in vitro permeation of ibuprofen in mammalian skin, the PAMPA model and silicone membrane.
644 *Int. J. Pharm.* 505, 14-19.

645 Merwe, D.v.d., Riviere, J.E., 2005. Effect of vehicles and sodium lauryl sulphate on xenobiotic
646 permeability and stratum corneum partitioning in porcine skin. *Toxicology* 206, 325-335.

647 Neupane, R., Boddu, S.H.S., Renukuntla, J., Babu, R.J., Tiwari, A.K., 2020. Alternatives to biological
648 skin in permeation studies: Current trends and possibilities. *Pharmaceutics* 12.

649 Oliveira, G., Beezer, A.E., Hadgraft, J., Lane, M.E., 2010. Alcohol enhanced permeation in model
650 membranes. Part I. Thermodynamic and kinetic analyses of membrane permeation. *Int. J. Pharm.*
651 393, 61-67.

652 Oliveira, G., Hadgraft, J., Lane, M.E., 2012. The influence of volatile solvents on transport across
653 model membranes and human skin. *Int. J. Pharm.* 435, 38-49.

654 Ottaviani, G., Martel, S., Carrupt, P.-A., 2006. Parallel artificial membrane permeability assay: A new
655 membrane for the fast prediction of passive human skin permeability. *J. Med. Chem.* 49, 3948-3954.

656 Pistollato, F., Madia, F., Corvi, R., Munn, S., Grignard, E., Paini, A., Worth, A., Bal-Price, A., Prieto, P.,
657 Casati, S., Berggren, E., Bopp, S.K., Zuang, V., 2021. Current EU regulatory requirements for the
658 assessment of chemicals and cosmetic products: challenges and opportunities for introducing new
659 approach methodologies. *Arch. Toxicol.* 95, 1867-1897.

660 Rahma, A., Lane, M.E., 2022. Skin Barrier Function in Infants: Update and Outlook. *Pharmaceutics* 14.
661 Rhein, L., Robbins, C., Fernee, K., 1986. Surfactant structure effects on swelling of isolated human
662 stratum corneum. *J. Soc. Cosmet. Chem.* 37, 125-139.

663 Riviere, J.E., Brooks, J.D., Yeatts, J.L., Koivisto, E.L., 2010. Surfactant effects on skin absorption of
664 model organic chemicals: implications for dermal risk assessment studies. *Journal of Toxicology and
665 Environmental Health A* 73, 725-737.

666 Salama, P., Gliksberg, A., Cohen, M., Tzafrir, I., Ziklo, N., 2021. Why are wet wipes so difficult to
667 preserve? Understanding the intrinsic causes. *Cosmetics* 8, 73.

668 Schmook, F.P., Meingassner, J.G., Billich, A., 2001. Comparison of human skin or epidermis models
669 with human and animal skin in in-vitro percutaneous absorption. *Int. J. Pharm.* 215, 51-56.

670 Sheehan, A.A., 2016. Non-wovens with high interfacial pore size and method of making same.
671 Google Patents.

672 Sheskey, P.J., Hancock, B.C., Moss, G.P., Goldfarb, D.J., 2020. Handbook of pharmaceutical
673 excipients, 9th ed. Pharmaceutical Press, S.I.

674 Shokri, J., Nokhodchi, A., Dashbolaghi, A., Hassan-Zadeh, D., Ghafourian, T., Barzegar Jalali, M., 2001.
675 The effect of surfactants on the skin penetration of diazepam. *Int. J. Pharm.* 228, 99-107.

676 Sinkó, B., Bárdos, V., Vestergombi, D., Kádár, S., Malcsiner, P., Moustie, A., Jouy, C., Takács-Novák,
677 K., Grégoire, S., 2021. Use of an in vitro skin parallel artificial membrane assay (Skin-pampa) as a
678 screening tool to compare transdermal permeability of model compound 4-phenylethyl-resorcinol
679 dissolved in different solvents. *Pharmaceutics* 13.

680 Sinkó, B., Garrigues, T.M., Balogh, G.T., Nagy, Z.K., Tsinman, O., Avdeef, A., Takács-Novák, K., 2012.
681 Skin-PAMPA: A new method for fast prediction of skin penetration. *Eur. J. Pharm. Sci.* 45, 698-707.

682 Školová, B., Janůšová, B., Zbytovská, J., Gooris, G., Bouwstra, J., Slepíčka, P., Berka, P., Roh, J., Palát,
683 K., Hrabálek, A., Vávrová, K., 2013. Ceramides in the Skin Lipid Membranes: Length Matters.
684 *Langmuir* 29, 15624-15633.

685 Stamatias, G.N., Bensaci, J., Greugny, E., Kaur, S., Wang, H., Dizon, M.V., Cork, M.J., Friedman, A.J.,
686 Oddos, T., 2021. A Predictive Self-Organizing Multicellular Computational Model of Infant Skin
687 Permeability to Topically Applied Substances. *J. Invest. Dermatol.* 141, 2049-2055.e2041.

688 Uchida, T., Kadhum, W.R., Kanai, S., Todo, H., Oshizaka, T., Sugibayashi, K., 2015. Prediction of skin
689 permeation by chemical compounds using the artificial membrane, Strat-M™. *Eur. J. Pharm. Sci.* 67,
690 113-118.

691 US Food and Drug Administration, 1994. Reviewer guidance – Validation of chromatographic
692 methods, in: Center for Drug Evaluation Research (Ed.), Rockville, MD.

693 Wang, K., Karlsson, G., Almgren, M., 1999. Aggregation Behavior of Cationic Fluorosurfactants in
694 Water and Salt Solutions. A CryoTEM Survey. *The Journal of Physical Chemistry B* 103, 9237-9246.

695 Yoshimatsu, H., Ishii, K., Konno, Y., Satsukawa, M., Yamashita, S., 2017. Prediction of human
696 percutaneous absorption from in vitro and in vivo animal experiments. *Int. J. Pharm.* 534, 348-355.

697 Zhang, Y., Lane, M.E., Hadgraft, J., Heinrich, M., Chen, T., Lian, G., Sinkó, B., 2019. A comparison of
698 the in vitro permeation of niacinamide in mammalian skin and in the Parallel Artificial Membrane
699 Permeation Assay (PAMPA) model. *Int. J. Pharm.* 556, 142-149.

700

1 A comparative study of the *in vitro* permeation of 2-
2 phenoxyethanol in the skin PAMPA model and mammalian skin

3 Annisa Rahma^{a,b,*}, Majella E. Lane^b, Bálint Sinkó^c

4 ^a School of Pharmacy, Institut Teknologi Bandung, Ganesa 10, Bandung 40132, Indonesia

5 ^b School of Pharmacy, University College London, 29 – 39 Brunswick Square, London WC1N 1AX,
6 United Kingdom

7 ^c Pion Inc., 10 Cook Street, Billerica, Massachusetts 01821, United States

8

9 * corresponding author

10

11 Email addresses: annisarahma@fa.itb.ac.id (A. Rahma), m.lane@ucl.ac.uk (M.E. Lane),

12 bsinko@pion-inc.com (B. Sinkó).

13 **Abstract**

14 For permeation studies that use excised skin, experimental data may show variability
15 associated with the use of biological tissues. As a consequence, achieving reproducible
16 results and data interpretation may be challenging. The skin parallel artificial membrane
17 permeability assay (skin PAMPA) model has been proposed as a high-throughput tool for
18 predicting skin permeation of chemicals. A number of skin cleansing wipe formulations for the
19 diaper area of infants contain 2-phenoxyethanol (PE) as a preservative and cetylpyridinium
20 chloride (CPC) as a surfactant with antimicrobial activity. However, information regarding
21 cutaneous absorption of PE and CPC in the scientific literatures is remarkably limited. The
22 main aim of the present study was to assess the suitability of the skin PAMPA model for
23 prediction of skin permeation of PE. A secondary aim was to investigate the influence of CPC
24 on the dermal absorption of PE. PE (1% w/w) was prepared in two vehicles, namely propylene
25 glycol (PG) and water-PG (WP). Permeability of PE was investigated *in vitro* using the skin
26 PAMPA membrane, porcine skin and human skin under finite dose conditions. The highest
27 permeation of PE was observed for the water-PG preparation with 0.2% w/w of CPC. This
28 finding was consistently observed in the skin PAMPA model and in Franz cell studies using
29 porcine skin and human skin. Permeation of CPC was not detected in the three permeation
30 models. However, permeation of PE increased significantly ($p < 0.05$) in the presence of CPC
31 compared with formulations without CPC. When comparing the skin PAMPA data and the
32 mammalian skin data for the cumulative amount of PE permeated, the r^2 values for PAMPA-
33 porcine skin and PAMPA-human skin were 0.84 and 0.89, respectively. The findings in this
34 study demonstrate the capability of the skin PAMPA model to differentiate between various
35 doses and formulations and are encouraging for further applications of this model as a high
36 throughput screening tool in topical formulation development.

37 **Keyword:** dermal absorption, PAMPA, porcine skin, human skin, preservative, surfactant.

38

39 **1. Introduction**

40 Dermal absorption of ingredients in topical formulations intended for infants has not been
41 widely studied. The importance of assessing skin permeation of such ingredients has recently
42 been reviewed (Rahma and Lane, 2022; Stamatias et al., 2021). Baby wipes are used regularly
43 in the infant population, and mainly comprise a high percentage of water (>90%),
44 preservative(s), and surfactant(s). Phenoxyethanol (PE) is the most commonly used
45 preservative ingredient in baby wipe formulations and is typically included at a concentration
46 of 0.5-1% w/v. PE has been shown to demonstrate significantly lower adsorption ($p < 0.05$) to
47 the fabric component of baby wipes in comparison with methylparaben (Endo et al., 2020). In

48 addition, PE (log P 1.2) has a comparatively higher aqueous solubility compared with other
 49 preservatives commonly used in topical preparations such as parabens and benzoic acid
 50 (Sheskey et al., 2020). These are important considerations for formulations with high water
 51 content such as baby wipes. Although PE is extensively used in baby wipe formulations
 52 (Salama et al., 2021), it has also been reported to act as a penetration enhancer (Ibrahim and
 53 Li, 2009; Ibrahim and Li, 2010). The haemolytic effects of PE have long been acknowledged
 54 (European Union Scientific Committee on Consumer Safety, 2016). Following oral
 55 administration, PE undergoes rapid first pass metabolism and is then converted into 2-
 56 phenoxyacetic acid (European Union Scientific Committee on Consumer Safety, 2016).
 57 Therefore, the systemic bioavailability of PE is very low (European Union Scientific Committee
 58 on Consumer Safety, 2016). By contrast, percutaneous absorption resulted in higher
 59 concentrations of PE in blood (Kim et al., 2015). In 2012, the French National Agency for the
 60 Safety of Medicines and Health Products (ANSM) submitted a risk assessment concerning
 61 the use of PE as a preservative ingredient in cosmetic formulations (French National Agency
 62 for the Safety of Medicines and Health Products, 2019). The ANSM proposed that PE should
 63 be excluded from topical formulations intended for the diaper area of infants and children aged
 64 under 3 years. The main reasons were the haematotoxicity and hepatotoxicity potential and
 65 insufficient margins of safety (MoS) for children under 3 years old (Dreno et al., 2019;
 66 European Union Scientific Committee on Consumer Safety, 2016).

67 Some baby wipe formulations also contain cetylpyridinium chloride (CPC), a quaternary
 68 surfactant with antimicrobial activity. For example, three commercial baby wipes listed in Table
 69 1 contain PE and CPC. To date there is no information in the published scientific literature
 70 regarding the skin permeation of PE in the presence of surfactant(s). Although several authors
 71 have reported skin permeation of PE these studies used rodent skin. Therefore, the
 72 experimental data cannot be extrapolated to humans (Lane, 2013).

73

74 Table 1. Commercial baby wipes containing PE and CPC

75

Ingredient list	Cussons baby wipes pure & gentle	Paseo baby wipes	Pigeon baby wipes
Water	*	*	*
PE	*	*	*

PG	*	*	
Polyhexamethylene biguanide		*	
Benzalkonium chloride			*
CPC	*	*	*
Croduret		*	
PEG-40 hydrogenated castor oil	*		
PPG-5-ceteth-20	*		
Sodium lactate	*		
Sodium citrate			*
Citric acid		*	*
Sodium benzoate			*
Disodium EDTA	*		
PEG-45 palm kernel glycerides	*		
Sodium lauryl sarcosinate	*	*	
<i>Olea europaea</i> fruit oil	*		
Cyclodextrin	*		
Methylparaben	*		
l-menthol	*		
Ethylparaben	*		
Butylparaben	*		
Propylparaben	*		
Polydimethylsiloxane	*		
Chamomile extract		*	

Perfume

*

Prunus serrulata

*

flower extract

76

77 Excised human skin is the most preferred tissue for *in vitro* skin permeation studies that
78 are intended to estimate results in human (Dick and Scott, 1992; Schmook et al., 2001). The
79 major challenges in using excised human skin are (1) difficulty in sourcing the skin samples
80 and (2) intra- and inter-specimen variability (Dick and Scott, 1992; Schmook et al., 2001). The
81 latter may also be problematic when interpreting the results from permeation studies (Oliveira
82 et al., 2010; Zhang et al., 2019). Porcine skin has been considered as an appropriate surrogate
83 for human skin, with reference to the close representation of the permeability properties of
84 porcine tissue to human skin compared to other animal models (Dick and Scott, 1992;
85 Schmook et al., 2001). However, porcine skin reportedly has a lower barrier function than
86 human skin (Barbero and Frasch, 2009; Schmook et al., 2001; Yoshimatsu et al., 2017). In
87 addition, ethical concerns over the use of animals in experiments is rising (Hopf et al., 2020;
88 Pistollato et al., 2021). In light of these challenges, there has been a growing interest in
89 exploring high throughput permeation models that are capable of generating reproducible data
90 that may be extrapolated to man (Zhang et al., 2019).

91 The skin Parallel Artificial Membrane Permeation Assay (PAMPA) model has been
92 developed for prediction of percutaneous absorption. The development of the skin PAMPA
93 membrane and its use as percutaneous absorption model was first described by Ottaviani et
94 al. (Ottaviani et al., 2006). The membrane composition was then refined by Sinkó et al. to
95 achieve better representation of the intercellular stratum corneum (SC) region (Sinkó et al.,
96 2012). The skin PAMPA membrane is essentially a filter substrate coated with synthetic lipids
97 (ceramides, free fatty acids, and cholesterol) arranged in a 96-well plate. Several studies
98 have reported positive correlations for the permeability parameters of compounds using the
99 skin PAMPA model and conventional *ex vivo* permeation studies (Balázs et al., 2016; Kovács
100 et al., 2021; Sinkó et al., 2021; Zhang et al., 2019). However, these studies only investigated
101 permeation of actives under infinite dose conditions.

102 It is important to assess skin permeation using clinically relevant doses, where the applied
103 dose represents the actual exposure “in use”. Clinically relevant doses demonstrated a finite
104 dose profile or “plateau” for *in vitro* permeation studies (Franz, 1975, 1983; Lehman, 2014).
105 This reflects the depletion of the applied dose of active over time (Franz, 1983; Lehman, 2014).
106 Most recently Zhang and co-workers reported that permeation data for niacinamide in the skin

107 PAMPA model correlated well with porcine and human skin *in vitro* studies under finite dose
108 conditions but not under infinite dose conditions (Zhang et al., 2019). Thus, the primary
109 objective of the present work was to investigate the suitability of the skin PAMPA model for
110 determination of dermal absorption of PE in the presence and absence of CPC in model
111 formulations. To this end, *in vitro* studies were conducted in the skin PAMPA model and in
112 porcine skin or human skin using Franz diffusion cells under finite dose conditions. A
113 secondary objective was to elucidate the influence of CPC on the dermal absorption of PE.

114

115 **2. Materials and Methods**

116 **2.1. Materials**

117 PE, CPC, and propylene glycol (PG) were purchased from Sigma-Aldrich Co., USA. HPLC
118 grade solvents (acetonitrile, methanol, water, and trifluoroacetic acid) were purchased from
119 Fischer Scientific, UK. Phosphate-buffered saline (PBS) tablets were purchased from Oxoid
120 Ltd., UK. Porcine ear skin was obtained from a local abattoir. Excised abdominal human skin
121 from a single donor was obtained from a tissue bank with informed consent and institutional
122 ethical approval (Research Ethics Committee reference 07/H1306/98). Skin specimens were
123 stored at -20 °C prior to use. The skin PAMPA sandwich plate, skin PAMPA collector plates,
124 standard hydration solution, stirring disks and Gut-Box™ were supplied by Pion Inc. Billerica,
125 USA.

126

127 **2.2. Methods**

128 **2.2.1. Preparation of test solutions**

129 PE solutions were prepared in the presence or absence of CPC, as shown in Table 2. PG
130 was chosen as a single solvent system, whereas water-PG 97:3 (WP) was chosen as a vehicle
131 that better represents the cleansing liquid in baby wipes. In addition, selected formulations
132 contained CPC either at 0.2% (w/w) or 1% (w/w). These concentrations represent the typical
133 concentration of surfactants used in baby wipes (Cunningham et al., 2008; Cunningham et al.,
134 2016; Sheehan, 2016). The full details of the formulations used in this study are listed in Table
135 2.

136

137

138

139

Table 2. PE solutions used in permeation studies.

Formulation	PE (% w/w)	CPC (% w/w)	Vehicle
PG1	1	-	PG
PG2	1	0.2	PG
PG3	1	1	PG
WP1	1	-	WP
WP2	1	0.2	WP
WP3	1	1	WP

140

141 The solutions were freshly prepared before the experiments. For PG2, PG3, WP2, and
142 WP3, mixing of the ingredients was performed with mild stirring to avoid foam formation by
143 CPC.

144

145 2.2.2. Skin PAMPA studies

146 *Influence of CPC on PAMPA membrane integrity*

147 In order to assess the compatibility of the skin PAMPA membrane with CPC, permeation
148 of CPC in the PAMPA model was monitored over 6 h. For these tests, CPC was dissolved in
149 PG at a final concentration of 0.2% w/w and 1% w/w. The permeation studies were performed
150 using the same setup as described in the previous section. Eight different doses were used,
151 covering finite and infinite conditions: 6, 10, 18, 30, 103, 515, 181, and 909 $\mu\text{g}/\text{cm}^2$. To achieve
152 these doses, CPC was applied at application volumes of 1, 3, 17, and 30 μL .

153

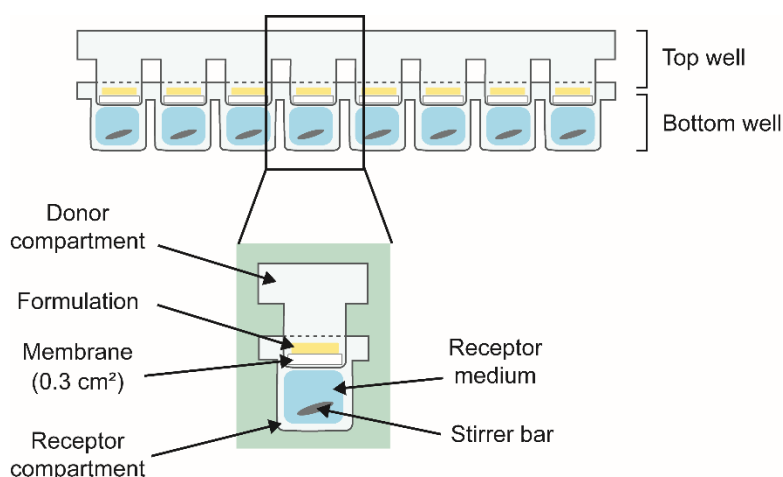
154 *Permeation of PE in the skin PAMPA membrane*

155 Permeability of PE was investigated in the skin PAMPA membrane using a modified
156 procedure reported by Luo et al. and Zhang et al. (Luo et al., 2016; Zhang et al., 2019). The
157 setup for this assay is illustrated in Fig. 1. The top side of the skin PAMPA sandwich plate was
158 set as the donor compartment, where the test solution was applied. For pilot studies, the dose
159 of PE applied was varied from 3 to 9 $\mu\text{L}/\text{cm}^2$ to assess the suitability of the experimental

160 design. Based on the results, an applied dose of $9 \mu\text{L}/\text{cm}^2$ was selected for the remaining
161 experiments.

162 The collector plates were added with stirring disks and filled with $180 \mu\text{l}$ of degassed
163 PBS ($\text{pH } 7.30 \pm 0.10$). Following application of the test solution, the two plates were assembled
164 and incubated in the Gut-Box™ stirring unit at $32 \pm 1 \text{ }^\circ\text{C}$ for 1 h. The collector plate was
165 replaced with a new plate prefilled with receptor solution at 1, 2, 5, 10, 15, 20, 30, 45, and 60
166 min.

167



168

169 **Fig. 1.** Experimental setup for skin PAMPA studies.

170

171 2.2.3. Franz cell studies

172 Skin permeation studies

173 Permeation studies were conducted using full-thickness porcine skin and heat-
174 separated human epidermis in Franz-type diffusion cells. Porcine skin was prepared as
175 described by Cristofoli et al. (Cristofoli et al., 2022). The epidermis of human skin was isolated
176 by the heat separation technique as described by Oliveira et al. (Oliveira et al., 2012). The
177 receptor medium was similar to that of the skin PAMPA assay. The permeation study was
178 conducted for 24 h at $32 \pm 1 \text{ }^\circ\text{C}$. Temperature was controlled by using a water bath (Sub Aqua
179 26 Plus, Grant™, Fischer Scientific, UK). Prior to the experiments, the skin impedance was
180 measured to assess the skin barrier integrity, as described previously (Oliveira et al., 2012).
181 The skin was then allowed to equilibrate to reach $32 \pm 1 \text{ }^\circ\text{C}$. The temperature of the skin was
182 measured using a digital thermometer (TM-22 Digitron, RS Components, UK). $10 \mu\text{L}$ of the
183 test solution, representing a finite dose of $10 \mu\text{L}/\text{cm}^2$ (corresponding to $100 \mu\text{g PE per cm}^2$),

184 was applied evenly on the donor compartment. 100 μ L of sample was withdrawn at 0, 0.5, 1,
185 2, 4, 6, 8, 10, 12, and 24 h. After sample collection, volume replacement was carried out by
186 adding 100 μ L of receptor solution (maintained at 32 ± 1 °C) to the receptor compartment. All
187 samples were analyzed for PE and CPC content using a validated HPLC method (section
188 2.2.4).

189

190 *Mass balance studies*

191 At the end of the permeation study, the receptor medium was immediately removed. Each
192 donor compartment was washed with 1 mL of methanol-water (85:15) mixture and the washing
193 solution was transferred to a 2 mL microcentrifuge tube. The cap of the tube was sealed with
194 Parafilm® to prevent evaporation. The washing procedure was performed 3 times. The Franz
195 diffusion cells were then disassembled, and each skin membrane was transferred to a 2 mL
196 microcentrifuge tube. 1 mL of methanol-water (85:15) was added to the microcentrifuge tube
197 and the cap of the tube was sealed with Parafilm® to prevent evaporation. Extraction of PE
198 and CPC was carried out by placing the tubes in a bench shaker (VWR International, USA) at
199 800 rpm for 12 h. All samples were centrifuged using an Eppendorf® microcentrifuge 5415R
200 (Eppendorf, UK) at 13,200 rpm for 20 min. Subsequently, the samples were analyzed for PE
201 and CPC content using a validated HPLC method. The percentage of the two ingredients
202 recovered from the washing solution, extraction solution, and the receptor solution was
203 determined.

204

205 *2.2.4. Quantification of PE and CPC*

206 The determination of PE and CPC content was performed using HPLC with a diode-array
207 detector (Agilent Technologies 1200 Series). Data acquisition was performed using
208 Chemstation software (Agilent Technologies, USA). A Kinetex® XB-C₁₈ column (250 x 4.60
209 mm, Phenomenex, UK) was used for the analysis. All the samples and standard solutions
210 were stored in amber HPLC vials during the assay. Optimized HPLC conditions were achieved
211 using a gradient elution system. The elution conditions are shown in Table 3. The flowrate,
212 injection volume, and column temperature were set as 1 ml/min, 20 μ L, and 40 °C,
213 respectively. The detection wavelengths were 258 nm (for CPC) and 270 nm (For PE).

214

215

216

217

Table 3. Elution conditions for PE and CPC.

Time	Volume ratio of mobile phase (%)	
	acetonitrile	0.1% TFA
	0 – 4	28
5 – 12	80	20
13 – 16	28	72

218

219 Validation of the analytical method was carried out in accordance with the guidelines
220 outlined by the International Conference on Harmonization (ICH) regarding quantitative
221 assays for determination of the content of active compounds (ICH Harmonised Tripartite,
222 2005). The following parameters were assessed: linearity, range, accuracy, intra-day and
223 inter-day precision, limit of detection (LOD), limit of quantification (LOQ), and robustness. In
224 addition, a system suitability test was performed to ensure that consistent chromatographic
225 behavior was achieved for each analytical procedure (US Food and Drug Administration,
226 1994).

227

228 2.2.5. Statistical analysis

229 Statistical analysis was performed using Origin 8.0 (OriginLab Corp., Northampton, MA).
230 Data were assessed for normal distribution and homogeneity using the Shapiro-Wilk Test and
231 Levene's Test, respectively. Sets of data that met the assumptions of normality and
232 homogeneity were analyzed using one-way ANOVA followed by Tukey's post hoc test. The
233 Kruskal–Wallis H Test was used for datasets that did not follow the assumptions of normality
234 and/or homogeneity of variance. The level of significance was set at a p-value lower than 0.05
235 ($p < 0.05$). The correlation assessment was performed using the Pearson correlation coefficient
236 (r^2).

237

238 3. Results

239 3.1. HPLC method validation

240 The results of method validation are shown in Table 4. The retention times of PE and CPC
241 using the validated method were 6.01 and 9.40 min, respectively. The linearity for PE and
242 CPC was obtained for a concentration range of 1 to 100 $\mu\text{g/mL}$. The calibration curve from

243 this range of concentrations exhibited a linear regression line. The LOD and LOQ for PE were
 244 calculated as 0.49 µg/mL and 1.49 µg/mL, respectively. The LOD and LOQ for CPC were 0.51
 245 µg/mL and 1.55 µg/mL, respectively.

246

247 **Table 4.** Summary of validation parameters for PE and CPC analysis using HPLC

Parameters	PE	CPC
Linearity range (µg/mL)	1 – 100	1 – 100
r ²	>0.99	>0.99
LOD (µg/mL)	0.49	0.51
LOQ (µg/mL)	1.49	1.55
Accuracy		
Recovery (%)	100.07 ± 0.34	100.42 ± 0.59
RSD (%)	0.03 – 0.65	0.04 – 0.89
Precision		
Intra-day (%RSD)	0.17	0.42
Inter-day (%RSD)	0.25	1.14
Robustness (r ²)	>0.99	>0.99
System suitability		
peak area (%RSD)	0.16	0.59
RT (%RSD)	0.10	0.10
Peak symmetry (%RSD)	0.99	0.18

248 RSD = relative standard deviation

249

250 The accuracy, which represents the closeness between the experimentally measured
 251 values and the true values, was determined by measuring the response of blank samples
 252 spiked with PE and CPC at 5, 50, and 100 µg/mL, representing the low, medium, and high
 253 concentrations. The average recovery value for PE was 100.07 ± 0.34 %, with a relative
 254 standard deviation (RSD) value <1%. As for CPC, the recovery value was 100.42 ± 0.59 %,
 255 with an RSD value <1.00%. The precision of the method was assessed based on intra-day
 256 and inter-day precision assessments. The RSD of the measured concentrations was used to
 257 express the inter-assay variability. Acceptable precision was achieved with corresponding
 258 RSD values of <1.00% and <2.00% for intra-day and inter-day assessment, respectively.

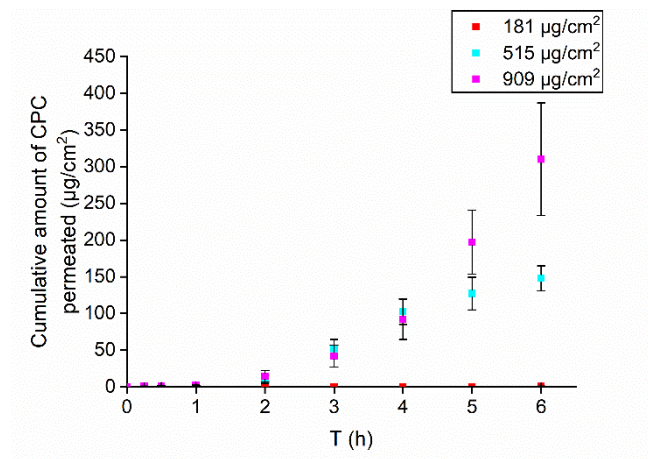
259 The robustness of an analytical method is investigated to ensure that the capability of
260 the HPLC system remains unaffected with minor variations in chromatographic conditions.
261 The robustness test was performed on standard solutions containing PE and CPC within a
262 concentration range of 1-100 $\mu\text{g/mL}$. Despite the minor variations (2% change) in injection
263 volume, flow rate, column temperature, mobile phase composition, and detection wavelength,
264 r^2 values remained ≥ 0.99 . A system suitability test was performed by determining the RSD of
265 the injection repeatability, as described in the Reviewer Guidance on Validation of
266 Chromatographic Methods (US Food and Drug Administration, 1994). Six injections of
267 solutions with PE and CPC at a concentration of 50 $\mu\text{g/mL}$ were determined for the peak area,
268 peak symmetry, and retention time. The RSD values for these parameters were $\leq 1.00\%$ for
269 PE and CPC.

270

271 3.2. Influence of CPC on PAMPA membrane integrity

272 Fig. 2 compares the amount of CPC permeated from different applied doses. When the
273 applied dose was $\leq 103 \mu\text{g/cm}^2$, permeation of CPC was not detected over 6 h. For the 181
274 $\mu\text{g/cm}^2$ dose, permeation of CPC was evident from 5 h. The amount of CPC permeated for
275 this dose was $0.06 \pm 0.07 \mu\text{g/cm}^2$ at 5 h. At the higher dose of CPC ($\geq 515 \mu\text{g/cm}^2$), the
276 permeation of CPC was observed at earlier timepoints.

277



278

279 **Fig. 2.** The amount of CPC permeated through the skin PAMPA membrane under various
280 applied doses (mean \pm SD, n = 6).

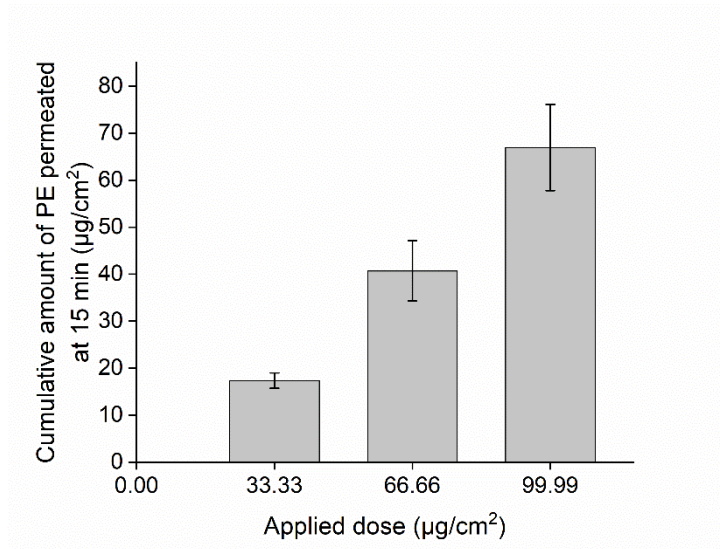
281

282

283 3.3. Permeation of PE in the skin PAMPA membrane

284 Cumulative amounts of PE permeated through the skin PAMPA membrane from different
285 applied doses are shown in Fig. 3. Three PE doses were used in this set of experiments – 1,
286 2, and 3 μL . These doses corresponded to 3, 6, and 9 $\mu\text{L}/\text{cm}^2$.

287



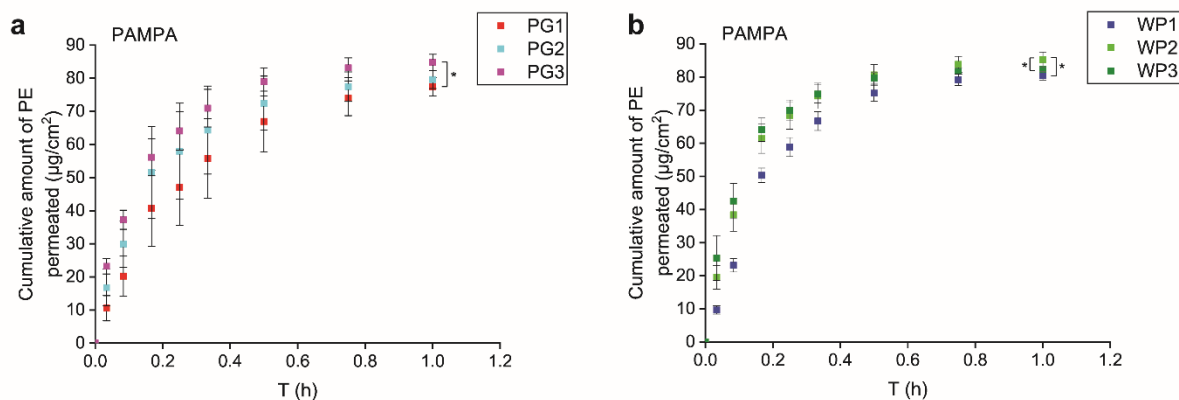
288

289 **Fig. 3.** Cumulative amounts of PE permeated through the skin PAMPA membrane from the
290 different applied doses (mean \pm SD, n = 6).

291

292 The permeation profiles of PE in the skin PAMPA model are shown in Fig. 4.
293 Permeation of PE was evident from 1 min. The highest permeation of PE was observed for
294 the solution containing CPC 0.2% with water-PG as the vehicle. The cumulative amount of PE
295 that permeated from this preparation was $85.30 \pm 2.19 \mu\text{g}/\text{cm}^2$. For preparations with neat PG
296 as the solvent, a significantly higher amount ($p < 0.05$) of PE permeated from the vehicle with
297 CPC 1%, compared with the PE solution with no CPC.

298



299

300 **Fig. 4.** Permeation profiles of PE from (a) PG and (b) Water-PG in the skin PAMPA
 301 membrane (mean \pm SD, n = 6). * Indicates statistical significance ($p < 0.05$) compared to the
 302 other preparations.

303

304 Interestingly, for water-PG preparations, the cumulative amount of PE permeated was
 305 significantly higher ($p < 0.05$) in the presence of CPC 0.2% compared with all other PE
 306 solutions. These findings suggested that the increase in PE permeation from water-PG was
 307 not necessarily proportional to the concentration of CPC.

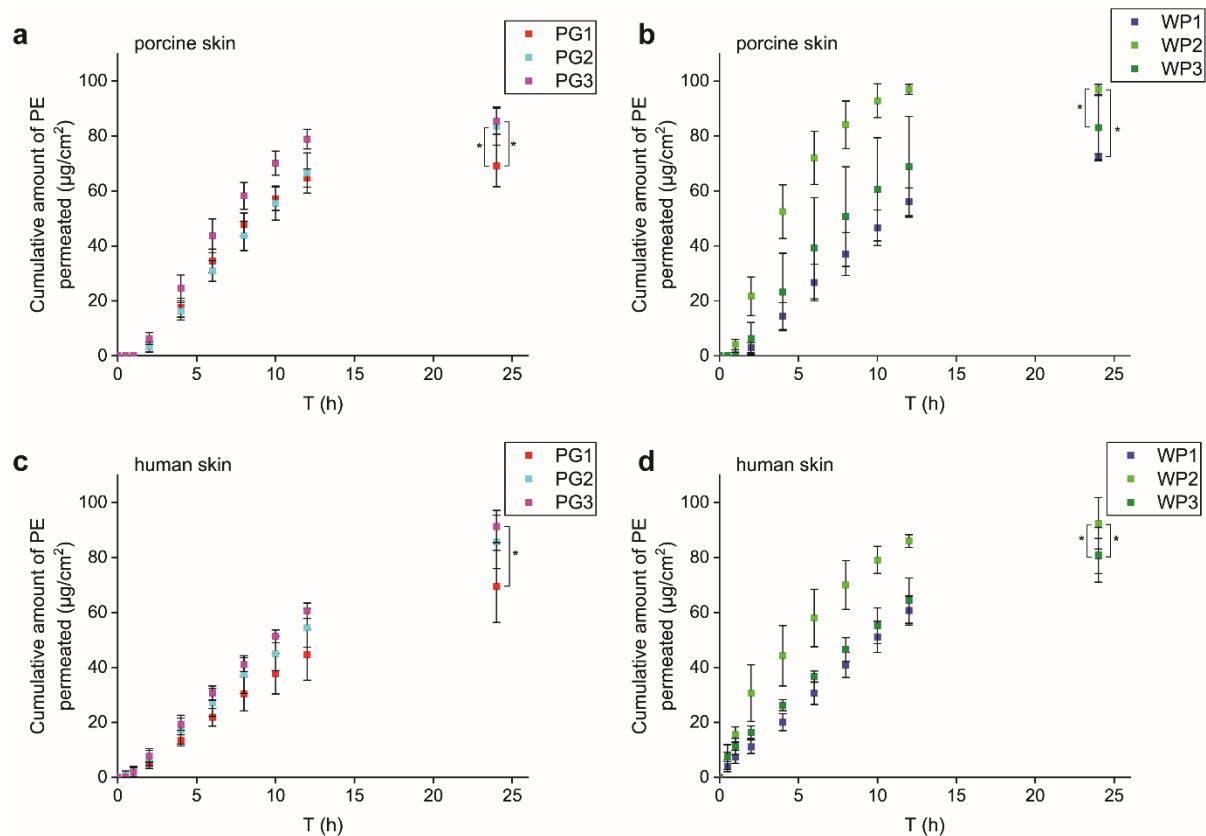
308

309 3.4. Franz cell studies

310 3.4.1. Permeation of PE in porcine skin and human skin

311 The permeation profiles of PE in porcine skin and human skin are shown in Fig. 5. We
 312 observed a trend which was consistent with the skin PAMPA data, where the highest
 313 permeation of PE was observed for water-PG with 0.2% of CPC. The cumulative amounts of
 314 PE that permeated in porcine skin and human skin from this preparation at 24 h were $96.98 \pm$
 315 $1.83 \mu\text{g}/\text{cm}^2$ and $92.46 \pm 9.34 \mu\text{g}/\text{cm}^2$, respectively. These values corresponded to more than
 316 97% of the applied dose. The lowest permeation of PE was observed for PG without CPC,
 317 both in porcine skin and human skin ($69.09 \pm 7.54 \mu\text{g}/\text{cm}^2$ and $73.99 \pm 9.70 \mu\text{g}/\text{cm}^2$,
 318 respectively). These results are consistent with the skin PAMPA data.

319



320

321 **Fig. 5.** Permeation profiles of PE from various preparations in porcine skin and human skin.
 322 (a) PG vehicle applied to porcine skin; (b) Water-PG vehicle applied to porcine skin; (c) PG
 323 vehicle applied to human skin; (d) Water-PG vehicle applied to human skin. Mean \pm SD, n =
 324 5-6. * Indicates statistical significance ($p < 0.05$) compared to the other preparations.

325

326 Regarding the effect of CPC on the permeation of PE, the results from porcine skin and
 327 human skin studies were consistent with the trends observed in the skin PAMPA studies. For
 328 PG, a significantly higher cumulative amount of PE permeation was evident in the presence
 329 of CPC 1% compared to preparations with no CPC ($p < 0.05$). This was observed both in
 330 porcine skin and human skin. For water-PG, the cumulative amount of PE permeated was
 331 significantly higher ($p < 0.05$) in the presence of CPC 0.2% compared with all other PE vehicles.

332

333 3.4.2. Mass balance studies for PE and CPC in porcine skin and human skin

334 The results of the mass balance studies for PE are shown in Table 5. The amount of PE
 335 that remained on the surface of porcine skin was a maximum of 2.01% of the applied dose for
 336 the PG vehicle. In contrast, PE was not detected in the washing solution for all water-PG
 337 preparations. For human skin data, the amount of PE that remained on the skin surface for

338 the PG vehicle was a maximum of 27.08% of the applied dose. Similar to the findings from
 339 porcine skin, PE was not detected in the washing solution for all water-PG preparations.
 340 Regarding the skin retention of PE, the percentages of the active recovered from the porcine
 341 skin for PG vehicle were 8.19-9.37% of the applied dose. For the water-PG preparations, 8.61-
 342 13.25% of PE was retained in porcine skin. The percentages of PE retained in human skin
 343 were lower than in porcine skin. At the end of the permeation studies, 3.08–3.57% of PE from
 344 the PG preparations were recovered in human skin. For the water-PG preparations, the
 345 percentage of PE extracted from human skin was 1.10–1.27%.

346

347 **Table 5.** Mass balance results for PE in porcine skin and human skin (mean \pm SD, n = 5).

Preparation	PE recovered (% of applied dose)			
	Receptor fluid	Skin surface	Skin	Total recovery
Porcine skin				
PG1	81.32 \pm 6.03	1.47 \pm 1.09	9.20 \pm 2.44	92.00 \pm 4.97
PG2	85.23 \pm 5.22	2.01 \pm 0.57	9.37 \pm 0.98	96.61 \pm 4.96
PG3	92.51 \pm 3.39	ND	8.19 \pm 0.82	100.70 \pm 2.83
WP1	79.00 \pm 4.04	ND	13.25 \pm 2.99	92.25 \pm 1.77
WP2	95.81 \pm 9.45	ND	8.61 \pm 0.94	104.49 \pm 8.56
WP3	88.29 \pm 10.28	ND	10.06 \pm 2.86	98.36 \pm 13.14
Human skin				
PG1	71.40 \pm 12.62	27.08 \pm 8.17	3.57 \pm 0.12	102.06 \pm 4.65
PG2	83.63 \pm 2.48	11.17 \pm 3.09	3.41 \pm 0.28	98.23 \pm 0.64
PG3	97.34 \pm 3.59	4.24 \pm 3.82	3.08 \pm 0.55	104.67 \pm 0.73
WP1	89.07 \pm 2.75	ND	1.11 \pm 0.17	90.19 \pm 2.92
WP2	97.79 \pm 6.66	ND	1.10 \pm 0.16	98.89 \pm 6.68
WP3	87.90 \pm 7.05	ND	1.27 \pm 0.12	89.18 \pm 7.02

348 ND = not detected

349

350 In contrast to PE, permeation of CPC was not detected in porcine skin and human skin
 351 studies for all preparations, as was observed in the skin PAMPA model. Mass balance results
 352 using porcine skin (Table 6) showed that the amount of CPC that remained on the skin surface
 353 varied between 61.31 to 95.28% of the applied dose, whereas the amount of CPC retained in
 354 the skin was 10.28-38.72% of the applied dose. In contrast, mass balance studies using

355 human skin confirmed that more than 80% of the applied dose of CPC was recovered from
 356 the skin surface for all vehicles (Table 6).

357

358 **Table 6.** Mass balance results for CPC in porcine skin and human skin (mean \pm SD, n = 5).

Preparation	Receptor fluid	CPC recovered (% of applied dose)		
		Skin surface	Skin	Total recovery
Porcine skin				
PG2	ND	83.21 \pm 8.44	21.12 \pm 7.68	104.33 \pm 1.19
PG3	ND	95.28 \pm 4.29	10.28 \pm 4.45	105.57 \pm 0.16
WP2	ND	61.31 \pm 0.87	38.72 \pm 1.99	100.04 \pm 2.16
WP3	ND	82.71 \pm 3.25	13.00 \pm 2.52	95.71 \pm 2.28
Human skin				
PG2	ND	85.06 \pm 8.07	8.81 \pm 1.13	93.88 \pm 7.01
PG3	ND	91.40 \pm 14.03	3.33 \pm 3.00	94.74 \pm 11.48
WP2	ND	90.04 \pm 9.87	7.72 \pm 2.33	97.77 \pm 7.84
WP3	ND	89.92 \pm 7.25	1.71 \pm 91.64	91.64 \pm 8.13

359 ND = not detected

360

361 **3.5. Comparative evaluation of the permeation data**

362 Cumulative amounts of PE that permeated the skin PAMPA membranes, porcine skin, and
 363 human skin are shown in Fig. 6. Statistical differences in the amount of PE that permeated
 364 from various preparations were assessed within the same vehicles rather than all vehicles.
 365 This approach should provide a clearer insight into possible active-vehicle-membrane
 366 interactions.

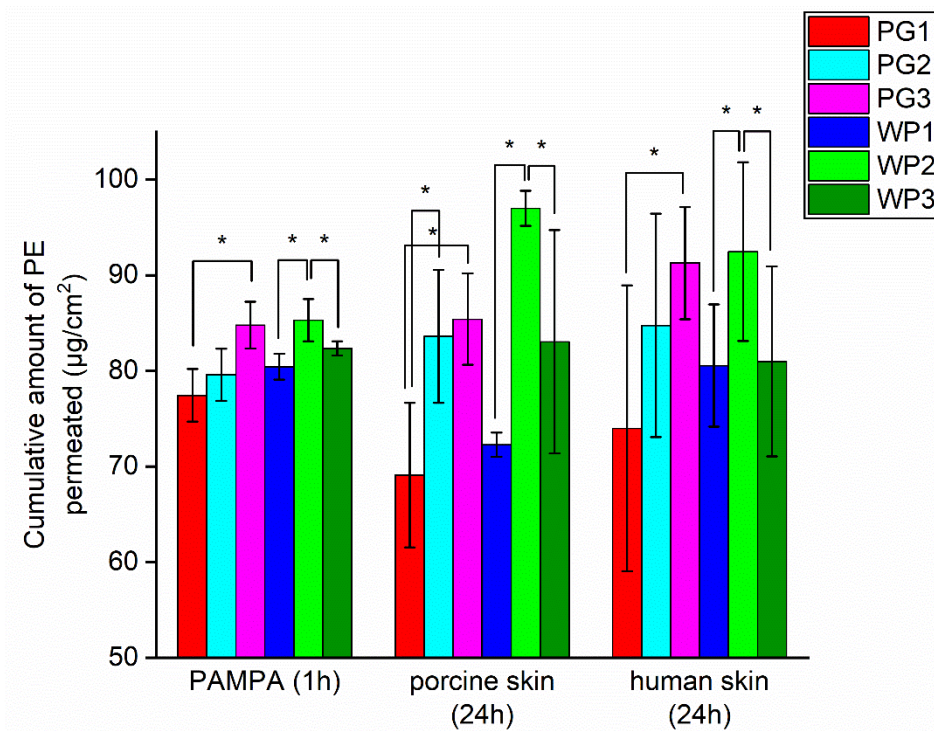
367

368

369

370

371



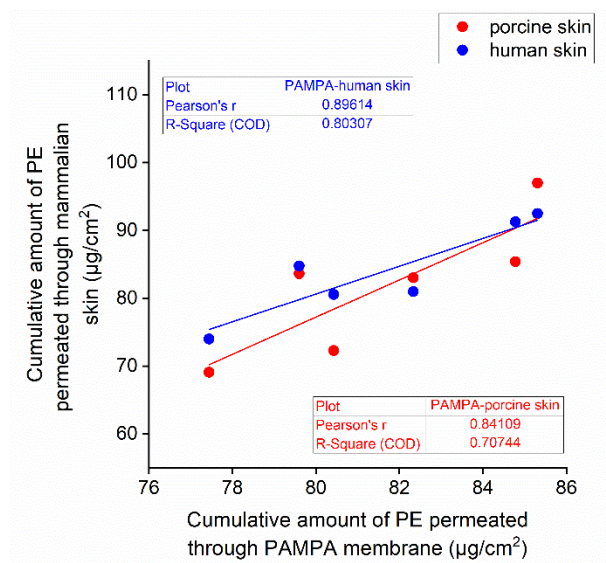
372

373 **Fig. 6.** Cumulative amounts of PE that permeated the membranes (mean ± SD, n = 5-6).

374 * Indicates statistical significance (p<0.05) compared to the other preparations within the
 375 same vehicle and within the same membrane model.

376

377 Correlations for the cumulative amount of PE permeated between the skin PAMPA data
 378 and the mammalian skin data are shown in Fig. 7. When comparing the skin PAMPA data and
 379 the porcine skin data for cumulative amount of PE permeated, the r^2 value was 0.84. This
 380 value is consistent with previously reported data by Zhang et al. (Zhang et al., 2019). For the
 381 correlation between the skin PAMPA and human skin data for cumulative amount of PE
 382 permeated the corresponding r^2 value was 0.89.



383

384

Fig. 7. Correlation between cumulative amounts of PE that permeated through skin PAMPA and mammalian skin. Each point represents the mean value (n = 5-6).

385

386

387

4. Discussion

388

389

390

391

392

393

394

395

396

397

398

399

400

401

402

403

404

405

406

Synthetic membranes mimicking the stratum corneum (SC) have been investigated extensively as surrogate models for *in vitro* skin permeation studies (Čuříková et al., 2017; de Jager et al., 2006b; Groen et al., 2011; Sinkó et al., 2012; Uchida et al., 2015). The membranes are composed of a porous substrate coated with synthetic SC lipids, which serve as the rate-determining barrier for skin permeation. In the present work, preliminary assessment of skin PAMPA compatibility with CPC was conducted prior to permeation studies for CPC-containing preparations. It is important to evaluate the compatibility of synthetic membranes with formulations, particularly when the formulation contains penetration enhancers (Köllmer et al., 2019; Kovács et al., 2021). Surfactants have been reported to have the potential to disrupt the organization of the SC lipids, although the mechanism underlying this is not fully understood (Gloor et al., 2004; Jiang et al., 2003). The interaction between surfactants and SC lipids is complex, depending on the duration of exposure, the nature, and the concentration of the surfactants (De la Maza et al., 1997; Imokawa, 2004; Rhein et al., 1986). Köllmer et al. recently investigated the compatibility of the skin PAMPA membrane with different surfactants (Köllmer et al., 2019). In their study, the skin PAMPA membrane was incubated with blank formulations which contained different surfactants (1% Brij™ S2 + 0.15% Brij™ S721 and 1% Brij™ S2 + 1% Brij™ S721). After 4 h of pre-incubation, a permeation test was performed for methylparaben, ethylparaben, and propylparaben for 4 h. The results indicated that pre-incubation with these surfactants did not increase the permeation of the parabens. In addition,

407 the rank order for permeation remained unchanged (methylparaben > ethylparaben >
408 propylparaben). The authors suggested that the surfactants used in the study did not alter the
409 permeability of the skin PAMPA membrane towards the parabens (Köllmer et al., 2019).

410 In the present study, permeation of CPC was not detected over 6 h when the application
411 dose was $\leq 103 \mu\text{g}/\text{cm}^2$. The concentration of CPC used in the permeation studies for PE-
412 containing vehicles using the skin PAMPA model was not more than $30 \mu\text{g}/\text{cm}^2$. In addition,
413 the duration of the experiment was only 1 h. Permeation of CPC from all vehicles was not
414 detected in the receptor solution over 1 h. More importantly, a comparison with the Franz cell
415 studies confirmed that the permeation data from the skin PAMPA model showed a good
416 correlation with the porcine skin and human skin data (Fig. 7). Therefore, no evident
417 incompatibility was observed between the skin PAMPA membrane with the vehicles used in
418 this study under previously mentioned conditions.

419 Possible membrane-excipient interactions such as membrane blockage by the
420 formulation, disorganization or solubilization of the membrane lipids have also been
421 recognized (Köllmer et al., 2019). Two recent studies reported the effects of several excipients
422 on the permeation of actives in the skin PAMPA membrane (Kovács et al., 2021; Zhang et al.,
423 2019). Zhang et al. reported that niacinamide permeated the skin PAMPA membrane from
424 PEG 400 and PEG 600, whereas it did not permeate in porcine and human skin studies (Zhang
425 et al., 2019). These authors suggested that this might reflect the interaction between those
426 solvents and the skin PAMPA membrane.

427 Finite dose experiments using the skin PAMPA model reported by Luo et al. and Zhang et
428 al. included application doses as low as $3 \mu\text{L}/\text{cm}^2$ (Luo et al., 2016; Zhang et al., 2019). These
429 studies reported comparable results for permeation profiles of the actives (ibuprofen,
430 niacinamide) between the skin PAMPA model and porcine skin as well as human skin. In the
431 current study, permeation of PE at the $3 \mu\text{L}/\text{cm}^2$ dose in the skin PAMPA membrane had
432 reached a plateau at 45 min. As frequent sampling within such a short period was impractical
433 and permeation data showed high variability, a dose of $9 \mu\text{L}/\text{cm}^2$ was selected as the final
434 dose for PE. As shown in Fig. 3, it is evident that by using the skin PAMPA model, a 1 h study
435 time was sufficient for PE to demonstrate comparable finite dose kinetics to those observed
436 in porcine skin and human skin in 24 h. Even with relatively high permeation of PE over a short
437 period, the skin PAMPA model was also capable of discriminating between different
438 preparations. This was reflected by the statistical differences between the formulations for the
439 cumulative amounts of PE permeated, as was observed in the porcine skin and human skin
440 studies (Fig. 6). Such high-throughput prediction in a time efficient manner is expected to be
441 particularly useful for screening numerous topical formulations (Luo et al., 2016; Neupane et

442 al., 2020; Sinkó et al., 2012; Zhang et al., 2019). Consistent with previously reported studies,
443 the time required for the active to permeate the artificial membrane was shorter compared with
444 porcine skin or human skin (Čuříková et al., 2017; Kovács et al., 2021; Luo et al., 2016; Zhang
445 et al., 2019). In addition, the variability in the skin PAMPA data, represented by the standard
446 deviation, was lower than in the Franz cell studies with mammalian tissue.

447 As shown in Fig. 4, the highest permeation of PE in the skin PAMPA model was observed
448 for water-PG with 0.2% of CPC. This finding was consistent with observations in the Franz cell
449 studies using porcine skin and human skin (Fig. 5). This concentration of CPC is typically used
450 in commercial baby wipe formulations, which comprise more than 90% of water and a low
451 concentration of surfactant (< 0.5%). On the other hand, the three permeation models
452 confirmed that the lowest permeation of PE was observed for neat PG without CPC. These
453 results also correspond with the findings from a study by Luo et al., where the highest amount
454 of active (ibuprofen) that permeated the skin PAMPA model was observed for the formulation
455 which delivered the highest amount of active in human skin under finite dose conditions (Luo
456 et al., 2016).

457 While permeation of CPC was not detected in the skin PAMPA model and Franz cell
458 studies, the presence of CPC enhanced the permeation of PE significantly ($p < 0.05$) compared
459 with preparations without CPC. Interestingly, better enhancement for permeation of PE was
460 observed when the CPC concentration was 1% for PG and 0.2% for water-PG. The results of
461 permeation studies using human skin showed that the cumulative amounts of PE permeated
462 from PG in the presence of CPC 0.2% and 1% were 14% and 23% higher, respectively,
463 compared with PE alone. For water-PG, the presence of CPC at 0.2% and 1% resulted in
464 enhanced PE permeation by 14% and 0.5%, respectively, compared to PE alone. This might
465 indicate that CPC influences the permeation of PE from PG and water-PG by different
466 mechanisms. In general, it has been thought that the alkyl chains of surfactants may
467 intercalate with the hydrophobic regions of the SC lipids (Gloor et al., 2004; Jiang et al., 2003).
468 The ability of surfactants to increase the permeation of various actives is well documented
469 (Merwe and Riviere, 2005; Riviere et al., 2010; Shokri et al., 2001). Clearly, it should be noted
470 that surfactants are able to form micelles, enhance the solubility of permeant and thus reduce
471 its thermodynamic activity (Lane, 2013). The critical micellar concentration of CPC was
472 reportedly 1 mM (approximately 0.34 mg/mL) in water at 25 °C (Wang et al., 1999). In the
473 present work, the concentrations of CPC used were 2 mg/mL and 10 mg/mL. For WP, the
474 vehicle with 97% water, CPC was present above the CMC which may explain the results
475 observed.

476 Regarding the correlation between the skin PAMPA data and mammalian skin data, the r^2
477 values for skin PAMPA-porcine skin and skin PAMPA-human skin were 0.84 and 0.89,
478 respectively (Fig. 7). Previously, Zhang et al. reported that the correlation for the permeation
479 of niacinamide between the skin PAMPA studies and porcine skin studies was 0.88 under
480 finite dose conditions. However, the corresponding r^2 value for human skin was lower
481 compared to porcine skin, namely 0.71.

482 It is important to note that artificial membranes are not intended to provide an estimation
483 of the amount of actives that permeate the human skin since these membranes do not fully
484 represent the biological complexity of human skin (Čuříková et al., 2017; Neupane et al.,
485 2020). Such models can be used as an initial screening tool before performing permeation
486 studies using human skin (Neupane et al., 2020; Zhang et al., 2019). Recently, a
487 comprehensive overview of the findings from permeation studies using synthetic membranes
488 was reported by Neupane et al. (Neupane et al., 2020). The main advantages of artificial
489 membranes are less variability in the thickness and composition compared with biological
490 tissues, and ease in storage (Neupane et al., 2020). A number of studies have demonstrated
491 the ability of artificial membranes to correlate with *ex vivo* permeation studies using porcine
492 skin or human skin (Balázs et al., 2016; Čuříková et al., 2017; de Jager et al., 2006a; Groen
493 et al., 2011; Sinkó et al., 2021; Sinkó et al., 2012; Uchida et al., 2015). However, most of the
494 studies were conducted under infinite dose conditions. On the other hand, finite dose
495 experiments are more relevant for prediction of dermal absorption with reference to the
496 amount of formulation applied in the real clinical setting. In finite dose experiments, the
497 implications of evaporation and residence time of the solvents, as well as the solubility of the
498 active in the remaining formulation should be taken into consideration (Lane, 2013).
499 Correlations observed in comparative studies using infinite dose conditions should not be
500 directly assumed to hold true for finite dose situations. As mentioned earlier, Zhang and co-
501 workers reported that the skin PAMPA data showed correlations with the porcine skin and
502 human skin data, for the amount of active permeated, under finite dose conditions but not
503 under infinite dose conditions (Zhang et al., 2019).

504 The importance of lipid composition for permeability of artificial membrane models has
505 been studied extensively. Groen et al. described the importance of lipid compositions
506 (cholesterol free fatty acid, and ceramide) for the permeability of skin lipid models (Groen et
507 al., 2011). In this study, the authors investigated the permeability of a stratum corneum
508 substitute (SCS) with various ratios of SC lipids. This was done by assessing the permeation
509 of benzoic acid under infinite dose conditions. It was found that the permeability of SCS to
510 benzoic acid was higher when the SCS membrane contained a high content of free fatty acids.
511 In contrast, permeation of benzoic acid was lower for SCS with high cholesterol or ceramide

512 content compared to SCS with equimolar composition of cholesterol free fatty acid, and
513 ceramide.

514 A synthetic ceramide named certramide is used in the skin PAMPA membrane (Sinkó et
515 al., 2012). Certramides are long-chain tartaric acid diamide derivatives. In the skin PAMPA
516 membrane, the length of the alkyl chains in the certramides are 8 and 18 (C8-C18). The
517 ceramides are combined with stearic acid and cholesterol (Sinkó et al., 2012). The ratio of the
518 membrane components in the skin PAMPA model was chosen to represent the intercellular
519 lipid matrix of the SC (Sinkó et al., 2012). The membrane demonstrated positive correlation
520 with human SC for permeation of various compounds (Sinkó et al., 2012). The effects of
521 molecular structure of ceramides on the permeability of a SC lipid model membrane have
522 previously been reported (Čuříková et al., 2017; Školová et al., 2013). Školová and co-workers
523 reported a decrease in permeability of the studied synthetic membrane for two drugs
524 (theophylline and indomethacin) when natural long-chain ceramides (24-acyl chains, Cer24)
525 were incorporated into the membrane compared to a control model without Cer24. Increased
526 permeation for both model compounds was observed when short-chain ceramides (4-6 acyl
527 chains) were used rather than the long-chain ceramides. Čuříková et al. investigated the
528 potential of simplified SC membranes to predict the effects of permeation enhancers on the
529 permeation of actives (Čuříková et al., 2017). This membrane model is composed of stearic
530 acid, cholesterol, cholesterol sulfate, and ceramides. The ceramides used in the study were
531 simplified, consisting of N-2-hydroxystearoyl phytosphingosine (CER[AP]) and/or N-stearoyl
532 phytosphingosine (CER[NP]), rather than more complex ceramides mixtures as developed
533 earlier by de Jager et al. (de Jager et al., 2006b). The optimized membrane, containing an
534 equimolar mixture of CER[AP] and CER[NP], was used to examine the permeation of two
535 active models, indomethacin and theophylline from formulations with different permeation
536 enhancers. For both actives, the enhancement of permeation by N-dodecyl azepan-2-one
537 (Azone) and (S)-N-acetylproline dodecyl ester (L-Pro2) observed in the membrane model was
538 consistent with porcine skin studies conducted under infinite dose conditions.

539

540 **5. Conclusions**

541 This work confirms the potential of the PAMPA model as a tool to discriminate between
542 different vehicles for permeation of actives. In addition, a positive correlation between the skin
543 PAMPA model and the Franz cell studies using porcine skin and human skin was observed
544 for the cumulative amount of PE permeated. Both the skin PAMPA model and Franz cell
545 studies using mammalian skin showed that the highest permeation of PE was observed for
546 CPC 0.2% in water-PG, which is the typical amount of CPC used in commercial baby wipe

547 formulations. Considering that skin cleansing using baby wipes is carried out regularly, the
548 findings of the current study may have implications for the safety evaluation of such products.
549 The three permeation models showed that the presence of CPC enhanced the permeation of
550 PE significantly ($p < 0.05$) compared with preparations without CPC. A greater enhancement
551 for permeation of PE was observed when the CPC concentration was 1% for PG and 0.2% for
552 water-PG. No evident incompatibilities between the skin PAMPA membrane and the examined
553 preparations were observed. Based on the present study and previous PAMPA publications it
554 is worth noting that the optimum experimental conditions for this model may vary for different
555 compounds. Future work will expand the range of actives to be studied in the model and further
556 investigate the application of the PAMPA model in high-throughput screening studies for
557 development of dermal formulations.

558

559

560 **Acknowledgement**

561 We thank our colleagues from the UCL Skin Research Group who provided insight and
562 expertise that greatly assisted the research. A.R. is grateful for financial support from The
563 Ministry of Finance of The Republic of Indonesia (Grant Ref: S-1778/LPDP.4/2019).

564

565 **Conflict of Interest**

566 The authors declare no conflict of interest.

567

568 **References**

- 569 Balázs, B., Vizserálek, G., Berkó, S., Budai-Szűcs, M., Kelemen, A., Sinkó, B., Takács-Novák, K., Szabó-
570 Révész, P., Csányi, E., 2016. Investigation of the Efficacy of Transdermal Penetration Enhancers
571 Through the Use of Human Skin and a Skin Mimic Artificial Membrane. *J. Pharm. Sci.* 105, 1134-1140.
- 572 Barbero, A.M., Frasc, H.F., 2009. Pig and guinea pig skin as surrogates for human in vitro
573 penetration studies: A quantitative review. *Toxicol. In Vitro* 23, 1-13.
- 574 Cristofoli, M., Hadgraft, J., Lane, M.E., Sil, B.C., 2022. A preliminary investigation into the use of
575 amino acids as potential ion pairs for diclofenac transdermal delivery. *Int. J. Pharm.* 623, 121906.
- 576 Cunningham, C., Mundschau, S., Seidling, J., Wenzel, S., 2008. Baby care, in: Schlossman, M. (Ed.),
577 The chemistry and manufacture of cosmetics, 2 ed. Allured, Chicago, pp. 1063-1154.
- 578 Cunningham, C.T., Seidling, J.R., Kroll, L.M., Mundschau, S.A., 2016. Stable emulsion for prevention
579 of skin irritation and articles using same. Google Patents.
- 580 Čuříková, B.A., Procházková, K., Filková, B., Diblíková, P., Svoboda, J., Kováčik, A., Vávrová, K.,
581 Zbytovská, J., 2017. Simplified stratum corneum model membranes for studying the effects of
582 permeation enhancers. *Int. J. Pharm.* 534, 287-296.
- 583 de Jager, M., Groenink, W., Bielsa i Guivernau, R., Andersson, E., Angelova, N., Ponec, M., Bouwstra,
584 J., 2006a. A Novel in Vitro Percutaneous Penetration Model: Evaluation of Barrier Properties with P-
585 Aminobenzoic Acid and Two of Its Derivatives. *Pharm. Res.* 23, 951-960.
- 586 de Jager, M., Groenink, W., van der Spek, J., Janmaat, C., Gooris, G., Ponec, M., Bouwstra, J., 2006b.
587 Preparation and characterization of a stratum corneum substitute for in vitro percutaneous
588 penetration studies. *Biochimica et Biophysica Acta (BBA) - Biomembranes* 1758, 636-644.
- 589 De la Maza, A., Coderch, L., Lopez, O., Baucells, J., Parra, J., 1997. Permeability changes caused by
590 surfactants in liposomes that model the stratum corneum lipid composition. *J. Am. Oil Chem. Soc.*
591 74, 1-8.
- 592 Dick, I.P., Scott, R.C., 1992. Pig Ear Skin as an In-vitro Model for Human Skin Permeability. *J. Pharm.*
593 *Pharmacol.* 44, 640-645.
- 594 Dreno, B., Zuberbier, T., Gelmetti, C., Gontijo, G., Marinovich, M., 2019. Safety review of
595 phenoxyethanol when used as a preservative in cosmetics. *J. Eur. Acad. Dermatol. Venereol.* 33, 15-
596 24.
- 597 Endo, Y., Mune, M., Usukura, J.U.N., 2020. Factors Affecting Reduction in Preservative Efficacy in
598 Nonwoven Fabrics. *Biocontrol Science* 25, 149-157.
- 599 European Union Scientific Committee on Consumer Safety, 2016. Opinion on Phenoxyethanol, in:
600 European Commission Health and Food Safety Directorate C: Public Health (Ed.).
- 601 Franz, T.J., 1975. Percutaneous absorption. On the relevance of in vitro data. *J. Invest. Dermatol.* 64,
602 190-195.
- 603 Franz, T.J., 1983. Kinetics of Cutaneous Drug Penetration. *Int. J. Dermatol.* 22, 499-505.

604 French National Agency for the Safety of Medicines and Health Products, 2019. Concentration of
605 phenoxyethanol in cosmetic products – Information statement.

606 Gloor, M., Wasik, B., Gehring, W., Grieshaber, R., Kleesz, P., Fluhr, J.W., 2004. Cleansing,
607 dehydrating, barrier-damaging and irritating hyperaemising effect of four detergent brands:
608 comparative studies using standardised washing models. *Skin Res. Technol.* 10, 1-9.

609 Groen, D., Poole, D.S., Gooris, G.S., Bouwstra, J.A., 2011. Investigating the barrier function of skin
610 lipid models with varying compositions. *Eur. J. Pharm. Biopharm.* 79, 334-342.

611 Hopf, N.B., Champmartin, C., Schenk, L., Berthet, A., Chedik, L., Du Plessis, J.L., Franken, A., Frasc,
612 F., Gaskin, S., Johanson, G., Julander, A., Kasting, G., Kilo, S., Larese Filon, F., Marquet, F., Midander,
613 K., Reale, E., Bunge, A.L., 2020. Reflections on the OECD guidelines for in vitro skin absorption
614 studies. *Regul. Toxicol. Pharmacol.* 117, 104752.

615 Ibrahim, S.A., Li, S.K., 2009. Effects of chemical enhancers on human epidermal membrane:
616 Structure-enhancement relationship based on maximum enhancement (E(max)). *J. Pharm. Sci.* 98,
617 926-944.

618 Ibrahim, S.A., Li, S.K., 2010. Chemical enhancer solubility in human stratum corneum lipids and
619 enhancer mechanism of action on stratum corneum lipid domain. *Int. J. Pharm.* 383, 89-98.

620 ICH Harmonised Tripartite, 2005. Validation of analytical procedures: text and methodology Q2 (R1),
621 International Conference on Harmonization, Geneva, Switzerland.

622 Imokawa, G., 2004. Surfactant-induced depletion of ceramides and other intercellular lipids:
623 implication for the mechanism leading to dehydration of the stratum corneum. *Exogenous*
624 *Dermatology* 3, 81-98.

625 Jiang, S.J., Zhou, X.J., Sun, G.Q., Zhang, Y., Jiang, S.J., Sun, G.Q., Zhang, Y., 2003. Morphological
626 alterations of the stratum corneum lipids induced by sodium lauryl sulfate treatment in hairless
627 mice. *J. Dermatol. Sci.* 32, 243-246.

628 Kim, T.H., Kim, M.G., Kim, M.G., Shin, B.S., Kim, K.-B., Lee, J.B., Paik, S.H., Yoo, S.D., 2015.
629 Simultaneous determination of phenoxyethanol and its major metabolite, phenoxyacetic acid, in rat
630 biological matrices by LC–MS/MS with polarity switching: Application to ADME studies. *Talanta* 144,
631 29-38.

632 Köllmer, M., Mossahebi, P., Sacharow, E., Gorissen, S., Gräfe, N., Evers, D., Herbig, M.E., 2019.
633 Investigation of the Compatibility of the Skin PAMPA Model with Topical Formulation and Acceptor
634 Media Additives Using Different Assay Setups. *AAPS PharmSciTech* 20.

635 Kovács, A., Zsikó, S., Falusi, F., Csányi, E., Budai-Szűcs, M., Csóka, I., Berkó, S., 2021. Comparison of
636 synthetic membranes to heat-separated human epidermis in skin permeation studies in vitro.
637 *Pharmaceutics* 13.

638 Lane, M.E., 2013. Skin penetration enhancers. *Int. J. Pharm.* 447, 12-21.

639 Lehman, P.A., 2014. A Simplified Approach for Estimating Skin Permeation Parameters from In Vitro
640 Finite Dose Absorption Studies. *J. Pharm. Sci.* 103, 4048-4057.

641 Luo, L., Patel, A., Sinko, B., Bell, M., Wibawa, J., Hadgraft, J., Lane, M.E., 2016. A comparative study of
642 the in vitro permeation of ibuprofen in mammalian skin, the PAMPA model and silicone membrane.
643 *Int. J. Pharm.* 505, 14-19.

644 Merwe, D.v.d., Riviere, J.E., 2005. Effect of vehicles and sodium lauryl sulphate on xenobiotic
645 permeability and stratum corneum partitioning in porcine skin. *Toxicology* 206, 325-335.

646 Neupane, R., Boddu, S.H.S., Renukuntla, J., Babu, R.J., Tiwari, A.K., 2020. Alternatives to biological
647 skin in permeation studies: Current trends and possibilities. *Pharmaceutics* 12.

648 Oliveira, G., Beezer, A.E., Hadgraft, J., Lane, M.E., 2010. Alcohol enhanced permeation in model
649 membranes. Part I. Thermodynamic and kinetic analyses of membrane permeation. *Int. J. Pharm.*
650 393, 61-67.

651 Oliveira, G., Hadgraft, J., Lane, M.E., 2012. The influence of volatile solvents on transport across
652 model membranes and human skin. *Int. J. Pharm.* 435, 38-49.

653 Ottaviani, G., Martel, S., Carrupt, P.-A., 2006. Parallel artificial membrane permeability assay: A new
654 membrane for the fast prediction of passive human skin permeability. *J. Med. Chem.* 49, 3948-3954.

655 Pistollato, F., Madia, F., Corvi, R., Munn, S., Grignard, E., Paini, A., Worth, A., Bal-Price, A., Prieto, P.,
656 Casati, S., Berggren, E., Bopp, S.K., Zuang, V., 2021. Current EU regulatory requirements for the
657 assessment of chemicals and cosmetic products: challenges and opportunities for introducing new
658 approach methodologies. *Arch. Toxicol.* 95, 1867-1897.

659 Rahma, A., Lane, M.E., 2022. Skin Barrier Function in Infants: Update and Outlook. *Pharmaceutics* 14.
660 Rhein, L., Robbins, C., Fernee, K., 1986. Surfactant structure effects on swelling of isolated human
661 stratum corneum. *J. Soc. Cosmet. Chem.* 37, 125-139.

662 Riviere, J.E., Brooks, J.D., Yeatts, J.L., Koivisto, E.L., 2010. Surfactant effects on skin absorption of
663 model organic chemicals: implications for dermal risk assessment studies. *Journal of Toxicology and
664 Environmental Health A* 73, 725-737.

665 Salama, P., Gliksberg, A., Cohen, M., Tzafrir, I., Ziklo, N., 2021. Why are wet wipes so difficult to
666 preserve? Understanding the intrinsic causes. *Cosmetics* 8, 73.

667 Schmook, F.P., Meingassner, J.G., Billich, A., 2001. Comparison of human skin or epidermis models
668 with human and animal skin in in-vitro percutaneous absorption. *Int. J. Pharm.* 215, 51-56.

669 Sheehan, A.A., 2016. Non-wovens with high interfacial pore size and method of making same.
670 Google Patents.

671 Sheskey, P.J., Hancock, B.C., Moss, G.P., Goldfarb, D.J., 2020. Handbook of pharmaceutical
672 excipients, 9th ed. Pharmaceutical Press, S.I.

673 Shokri, J., Nokhodchi, A., Dashbolaghi, A., Hassan-Zadeh, D., Ghafourian, T., Barzegar Jalali, M., 2001.
674 The effect of surfactants on the skin penetration of diazepam. *Int. J. Pharm.* 228, 99-107.

675 Sinkó, B., Bárdos, V., Vestergombi, D., Kádár, S., Malcsiner, P., Moustie, A., Jouy, C., Takács-Novák,
676 K., Grégoire, S., 2021. Use of an in vitro skin parallel artificial membrane assay (Skin-pampa) as a
677 screening tool to compare transdermal permeability of model compound 4-phenylethyl-resorcinol
678 dissolved in different solvents. *Pharmaceutics* 13.

679 Sinkó, B., Garrigues, T.M., Balogh, G.T., Nagy, Z.K., Tsinman, O., Avdeef, A., Takács-Novák, K., 2012.
680 Skin-PAMPA: A new method for fast prediction of skin penetration. *Eur. J. Pharm. Sci.* 45, 698-707.

681 Školová, B., Janůšová, B., Zbytovská, J., Gooris, G., Bouwstra, J., Slepíčka, P., Berka, P., Roh, J., Palát,
682 K., Hrabálek, A., Vávrová, K., 2013. Ceramides in the Skin Lipid Membranes: Length Matters.
683 *Langmuir* 29, 15624-15633.

684 Stamatias, G.N., Bensaci, J., Greugny, E., Kaur, S., Wang, H., Dizon, M.V., Cork, M.J., Friedman, A.J.,
685 Oddos, T., 2021. A Predictive Self-Organizing Multicellular Computational Model of Infant Skin
686 Permeability to Topically Applied Substances. *J. Invest. Dermatol.* 141, 2049-2055.e2041.

687 Uchida, T., Kadhum, W.R., Kanai, S., Todo, H., Oshizaka, T., Sugibayashi, K., 2015. Prediction of skin
688 permeation by chemical compounds using the artificial membrane, Strat-M™. *Eur. J. Pharm. Sci.* 67,
689 113-118.

690 US Food and Drug Administration, 1994. Reviewer guidance – Validation of chromatographic
691 methods, in: Center for Drug Evaluation Research (Ed.), Rockville, MD.

692 Wang, K., Karlsson, G., Almgren, M., 1999. Aggregation Behavior of Cationic Fluorosurfactants in
693 Water and Salt Solutions. A CryoTEM Survey. *The Journal of Physical Chemistry B* 103, 9237-9246.

694 Yoshimatsu, H., Ishii, K., Konno, Y., Satsukawa, M., Yamashita, S., 2017. Prediction of human
695 percutaneous absorption from in vitro and in vivo animal experiments. *Int. J. Pharm.* 534, 348-355.

696 Zhang, Y., Lane, M.E., Hadgraft, J., Heinrich, M., Chen, T., Lian, G., Sinkó, B., 2019. A comparison of
697 the in vitro permeation of niacinamide in mammalian skin and in the Parallel Artificial Membrane
698 Permeation Assay (PAMPA) model. *Int. J. Pharm.* 556, 142-149.

699

Table 1. Commercial baby wipes containing PE and CPC

<u>Ingredient list</u>	<u>Cussons baby wipes pure & gentle</u>	<u>Paseo baby wipes</u>	<u>Pigeon baby wipes</u>
<u>Water</u>	* -	* -	* -
<u>PE</u>	* -	* -	* -
<u>PG</u>	* -	* -	
<u>Polyhexamethylene biguanide</u>		* -	
<u>Benzalkonium chloride</u>			* -
<u>CPC</u>	* -	* -	* -
<u>Croduret</u>		* -	
<u>PEG-40 hydrogenated castor oil</u>	* -		
<u>PPG-5-ceteth-20</u>	* -		
<u>Sodium lactate</u>	* -		
<u>Sodium citrate</u>			* -
<u>Citric acid</u>		* -	* -
<u>Sodium benzoate</u>			* -
<u>Disodium EDTA</u>	* -		
<u>PEG-45 palm kernel glycerides</u>	* -		
<u>Sodium lauryl sarcosinate</u>	* -	* -	
<u>Olea europaea fruit oil</u>	* -		
<u>Cyclodextrin</u>	* -		
<u>Methylparaben</u>	* -		

l-menthol

*
-

Ethylparaben

*
-

Butylparaben

*
-

Propylparaben

*
-

Polydimethylsiloxane

*
-

Chamomile extract

*
-

Perfume

*
-

Prunus serrulata

flower extract

*
-

Table 12. PE solutions used in permeation studies.

Formulation	PE (% w/w)	CPC (% w/w)	Vehicle
PG1	1	-	PG
PG2	1	0.2	PG
PG3	1	1	PG
WP1	1	-	WP
WP2	1	0.2	WP
WP3	1	1	WP

Table 23. Elution conditions for PE and CPC.

Time	Volume ratio of mobile phase (%)	
	acetonitrile	0.1% TFA
	0 – 4	28
5 – 9	80	20
10 – 12	28	30
13 – 16	28	72

Table 34. Summary of validation parameters for PE and CPC analysis using HPLC

Parameters	PE	CPC
Linearity range ($\mu\text{g/mL}$)	1 – 100	1 – 100
r^2	>0.99	>0.99
LOD ($\mu\text{g/mL}$)	0.49	0.51
LOQ ($\mu\text{g/mL}$)	1.49	1.55
Accuracy		
Recovery (%)	100.07 \pm 0.34	100.42 \pm 0.59
RSD (%)	0.03 – 0.65	0.04 – 0.89
Precision		
Intra-day (%RSD)	0.17	0.42
Inter-day (%RSD)	0.25	1.14
Robustness (r^2)	>0.99	>0.99
System suitability		
peak area (%RSD)	0.16	0.59
RT (%RSD)	0.10	0.10
Peak symmetry (%RSD)	0.99	0.18

RSD = relative standard deviation

Table 45. Mass balance results for PE in porcine skin and human skin (mean \pm SD, n = 5).

Preparation	PE recovered (% of applied dose)			
	Receptor fluid	Skin surface	Skin	Total recovery
Porcine skin				
PG1	81.32 \pm 6.03	1.47 \pm 1.09	9.20 \pm 2.44	92.00 \pm 4.97
PG2	85.23 \pm 5.22	2.01 \pm 0.57	9.37 \pm 0.98	96.61 \pm 4.96
PG3	92.51 \pm 3.39	ND	8.19 \pm 0.82	100.70 \pm 2.83
WP1	79.00 \pm 4.04	ND	13.25 \pm 2.99	92.25 \pm 1.77
WP2	95.81 \pm 9.45	ND	8.61 \pm 0.94	104.49 \pm 8.56
WP3	88.29 \pm 10.28	ND	10.06 \pm 2.86	98.36 \pm 13.14
Human skin				
PG1	71.40 \pm 12.62	27.08 \pm 8.17	3.57 \pm 0.12	102.06 \pm 4.65
PG2	83.63 \pm 2.48	11.17 \pm 3.09	3.41 \pm 0.28	98.23 \pm 0.64
PG3	97.34 \pm 3.59	4.24 \pm 3.82	3.08 \pm 0.55	104.67 \pm 0.73
WP1	89.07 \pm 2.75	ND	1.11 \pm 0.17	90.19 \pm 2.92
WP2	97.79 \pm 6.66	ND	1.10 \pm 0.16	98.89 \pm 6.68
WP3	87.90 \pm 7.05	ND	1.27 \pm 0.12	89.18 \pm 7.02

ND = not detected

Table 56. Mass balance results for CPC in porcine skin and human skin (mean \pm SD, n = 5).

Preparation	CPC recovered (% of applied dose)			
	Receptor fluid	Skin surface	Skin	Total recovery
Porcine skin				
PG2	ND	83.21 \pm 8.44	21.12 \pm 7.68	104.33 \pm 1.19
PG3	ND	95.28 \pm 4.29	10.28 \pm 4.45	105.57 \pm 0.16
WP2	ND	61.31 \pm 0.87	38.72 \pm 1.99	100.04 \pm 2.16
WP3	ND	82.71 \pm 3.25	13.00 \pm 2.52	95.71 \pm 2.28
Human skin				
PG2	ND	85.06 \pm 8.07	8.81 \pm 1.13	93.88 \pm 7.01
PG3	ND	91.40 \pm 14.03	3.33 \pm 3.00	94.74 \pm 11.48
WP2	ND	90.04 \pm 9.87	7.72 \pm 2.33	97.77 \pm 7.84
WP3	ND	89.92 \pm 7.25	1.71 \pm 91.64	91.64 \pm 8.13

ND = not detected

Fig. 1

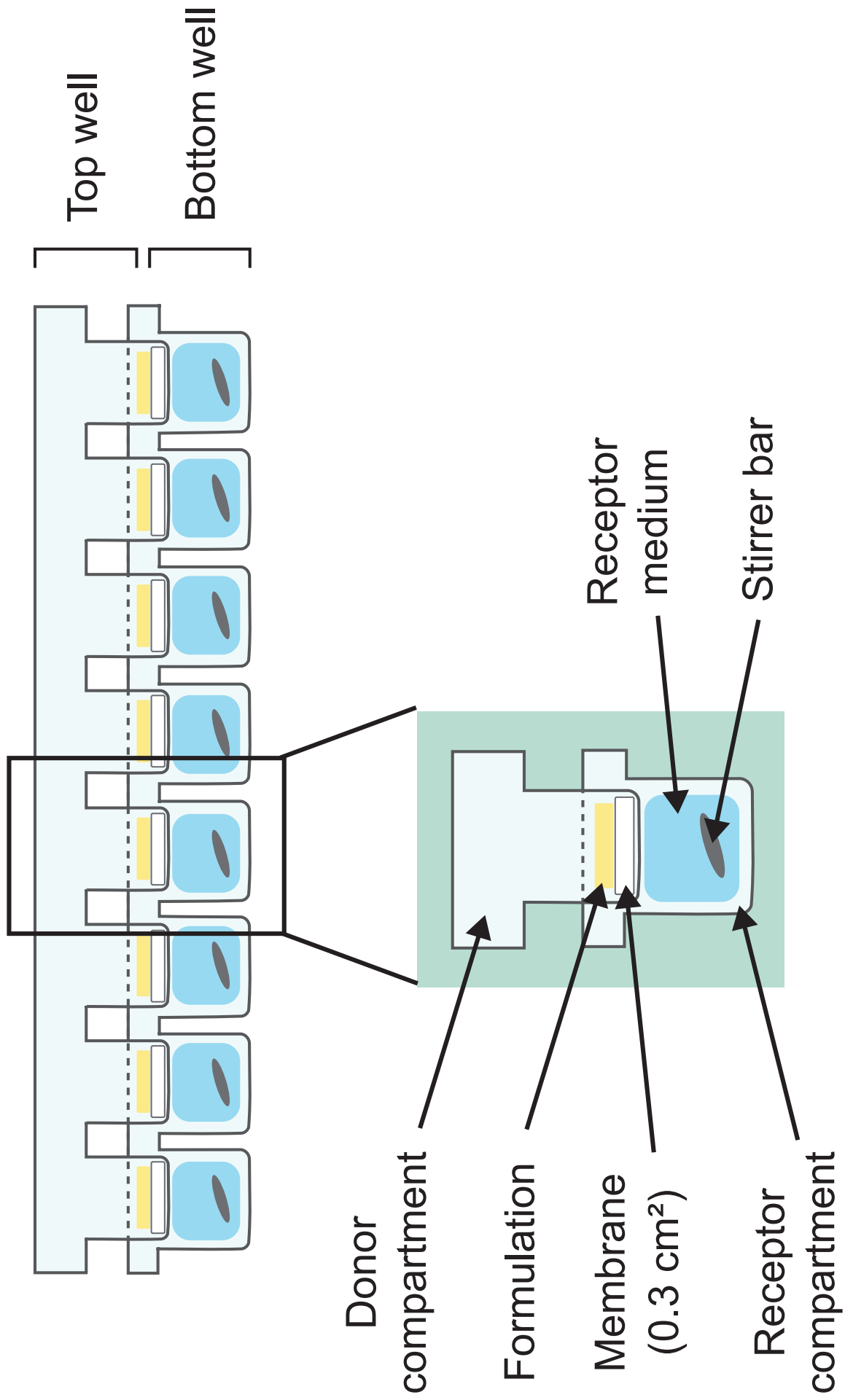


Fig. 2

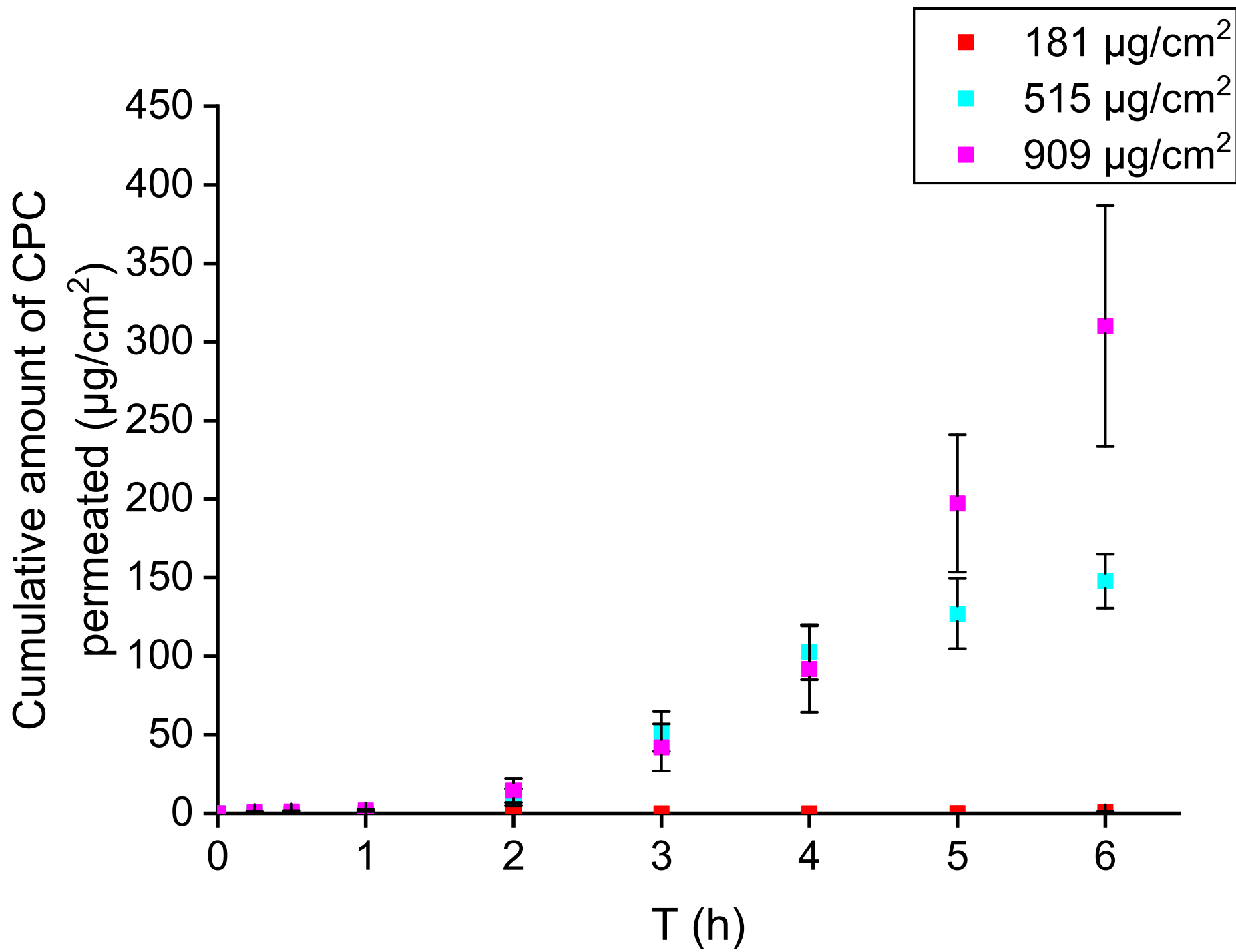


Fig. 3

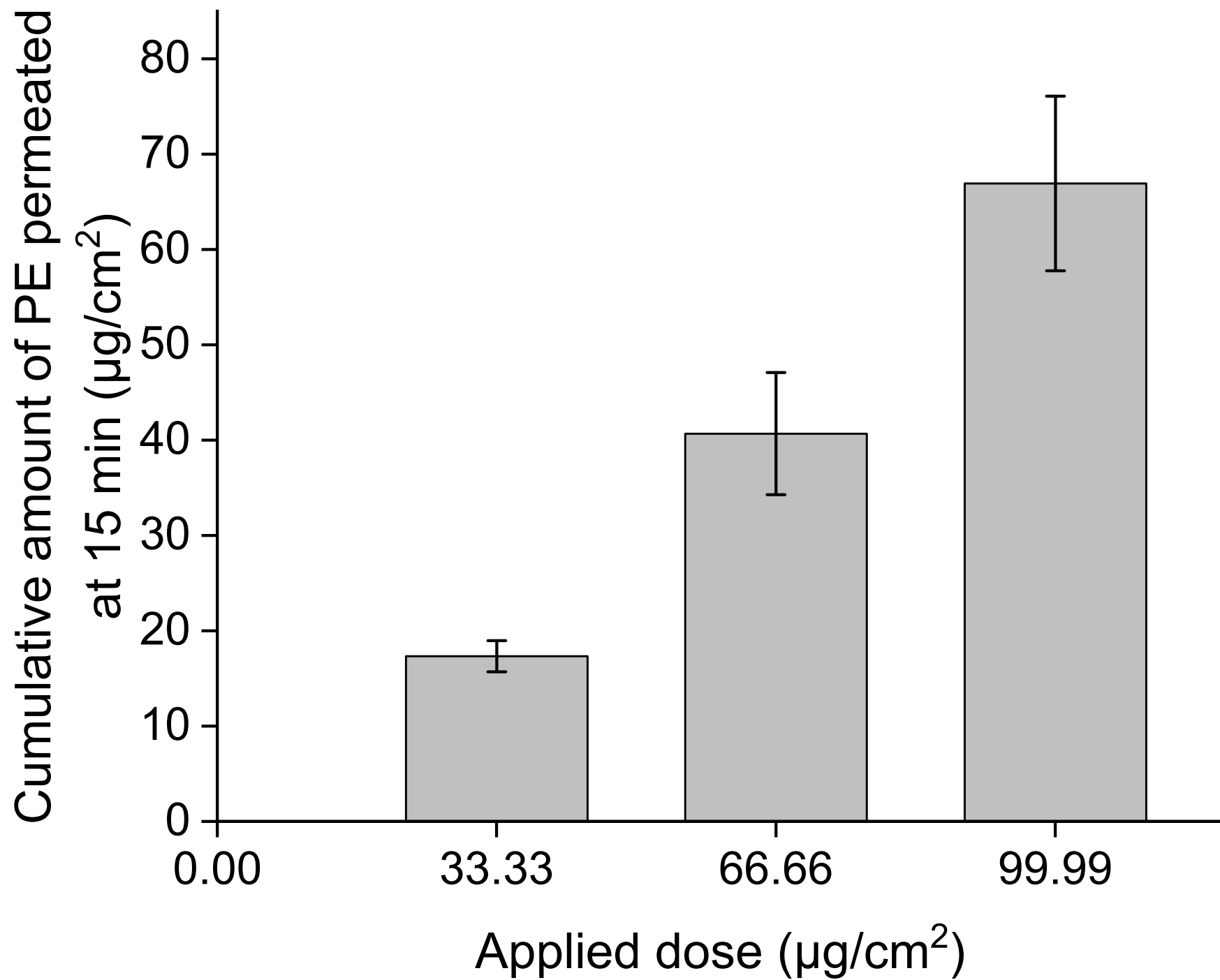


Fig. 4

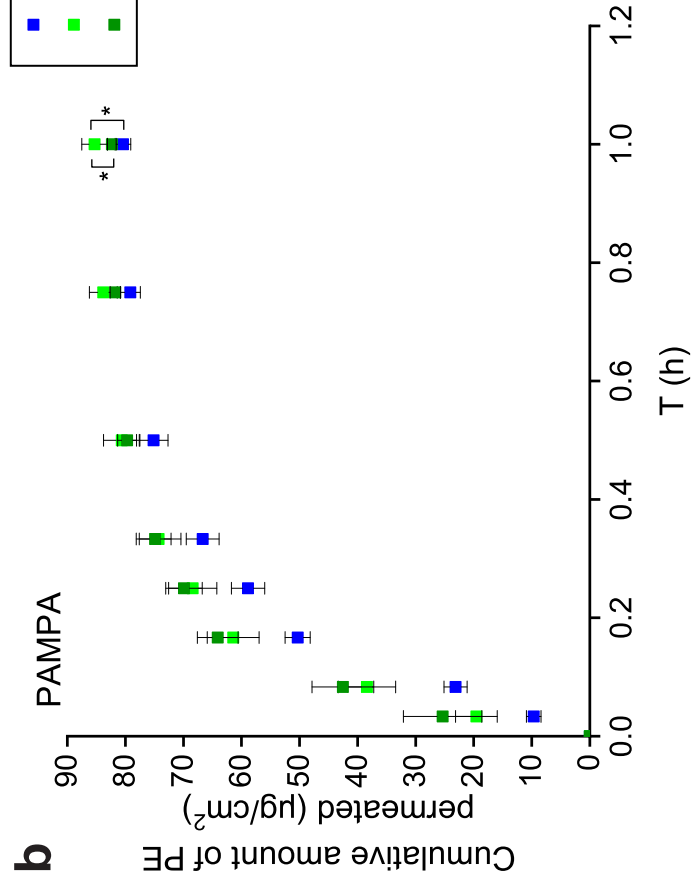
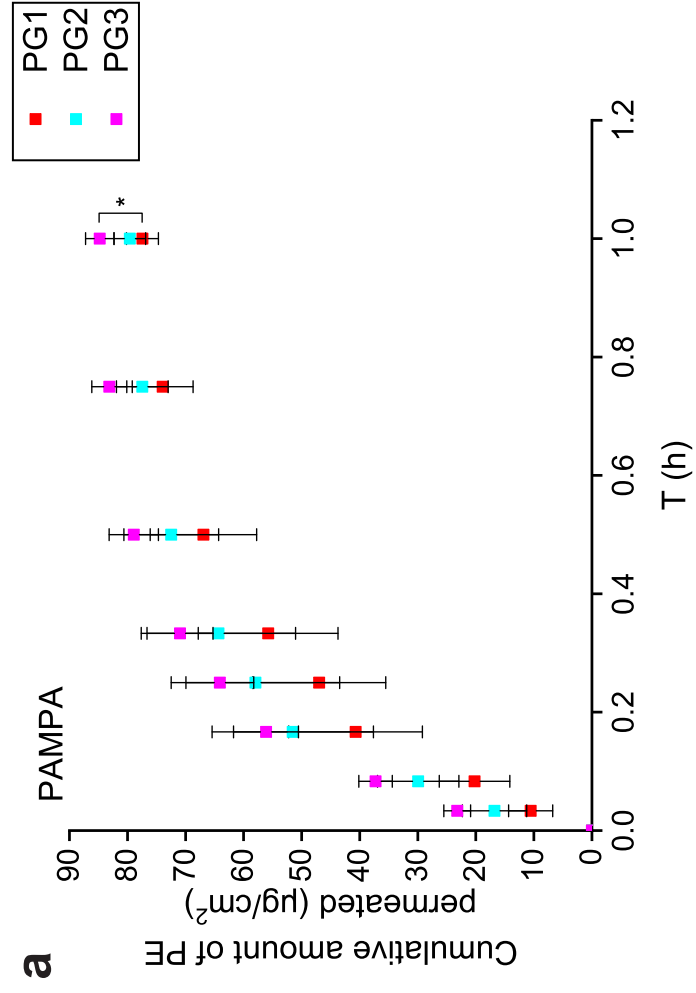


Fig. 5

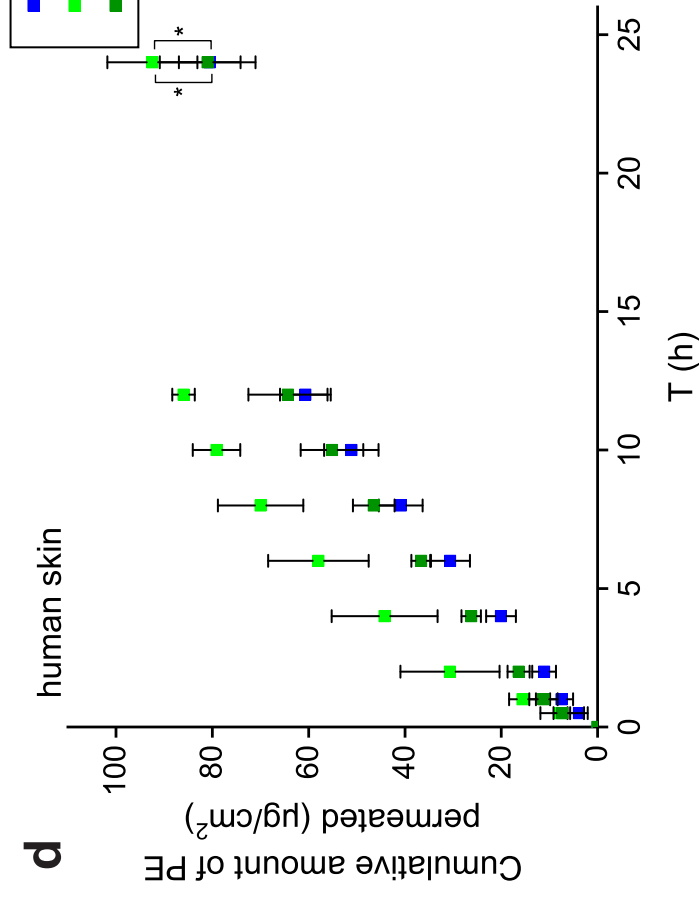
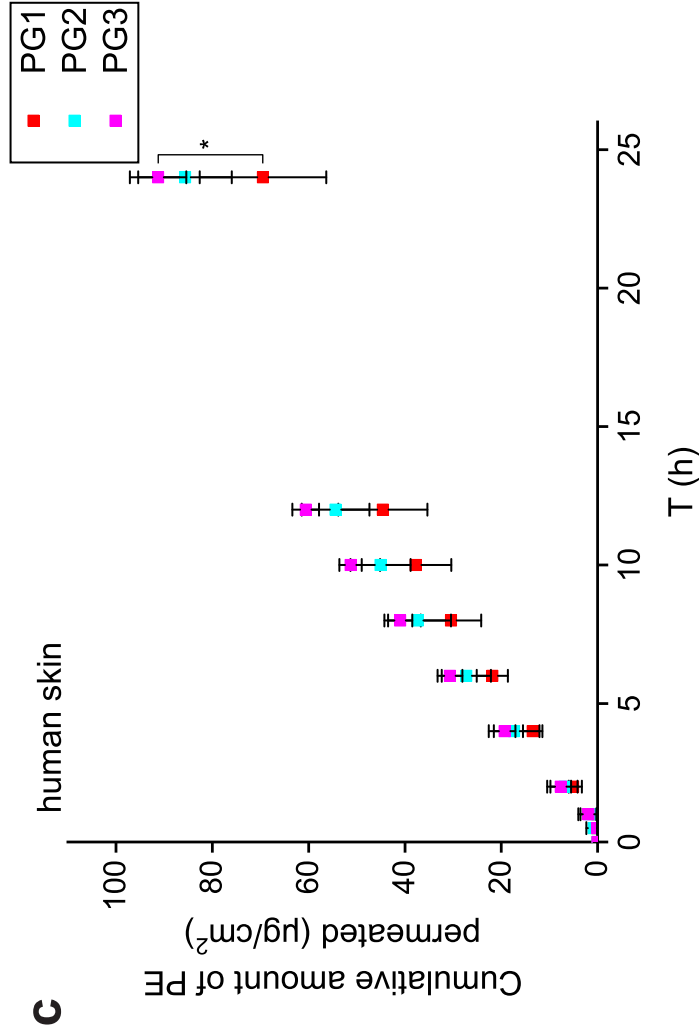
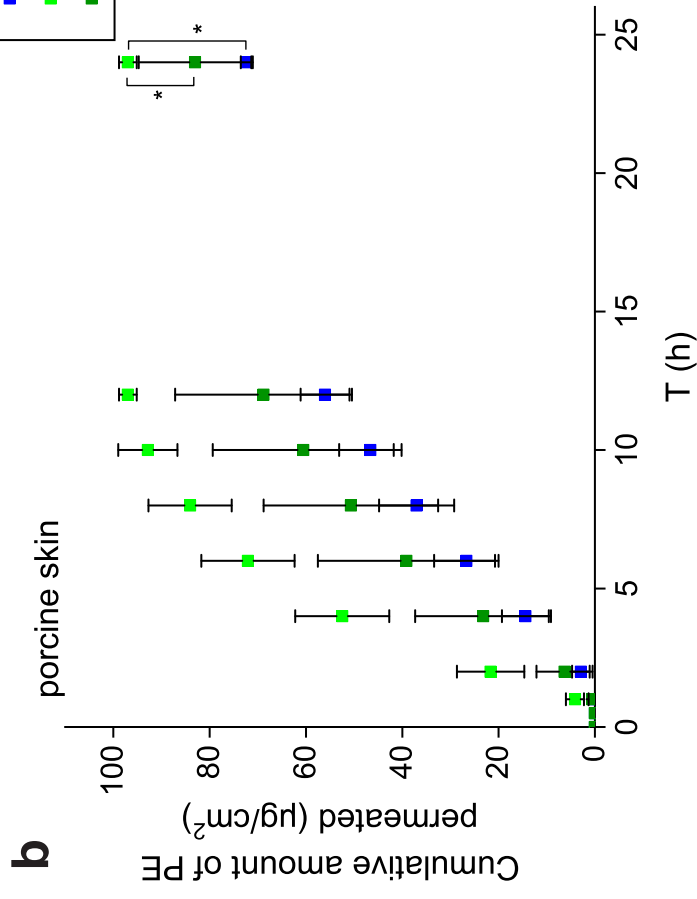
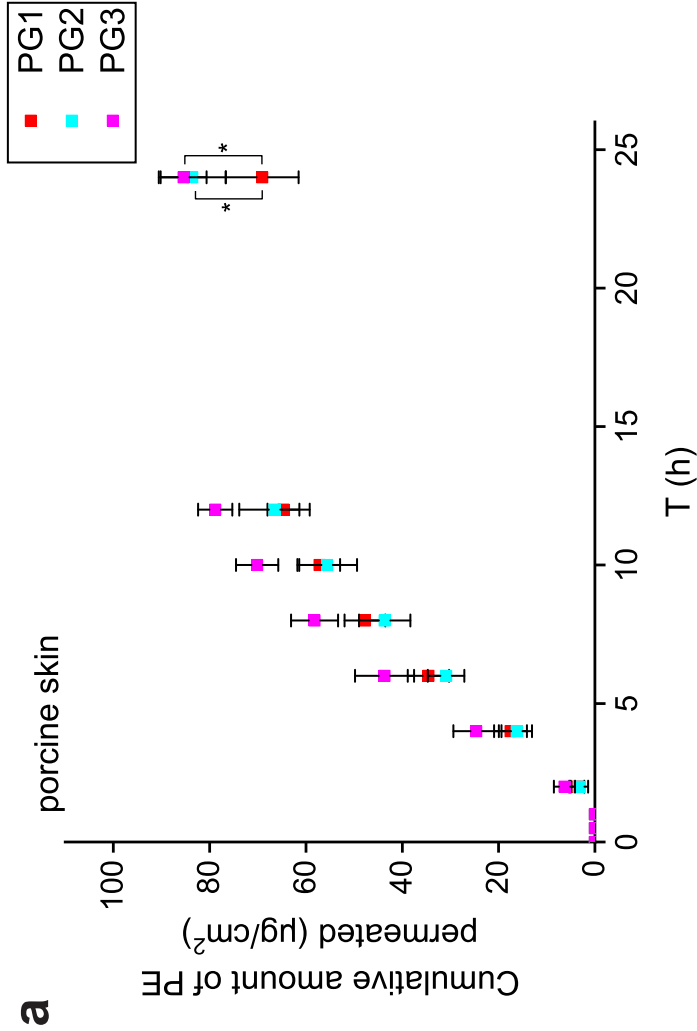


Fig. 6

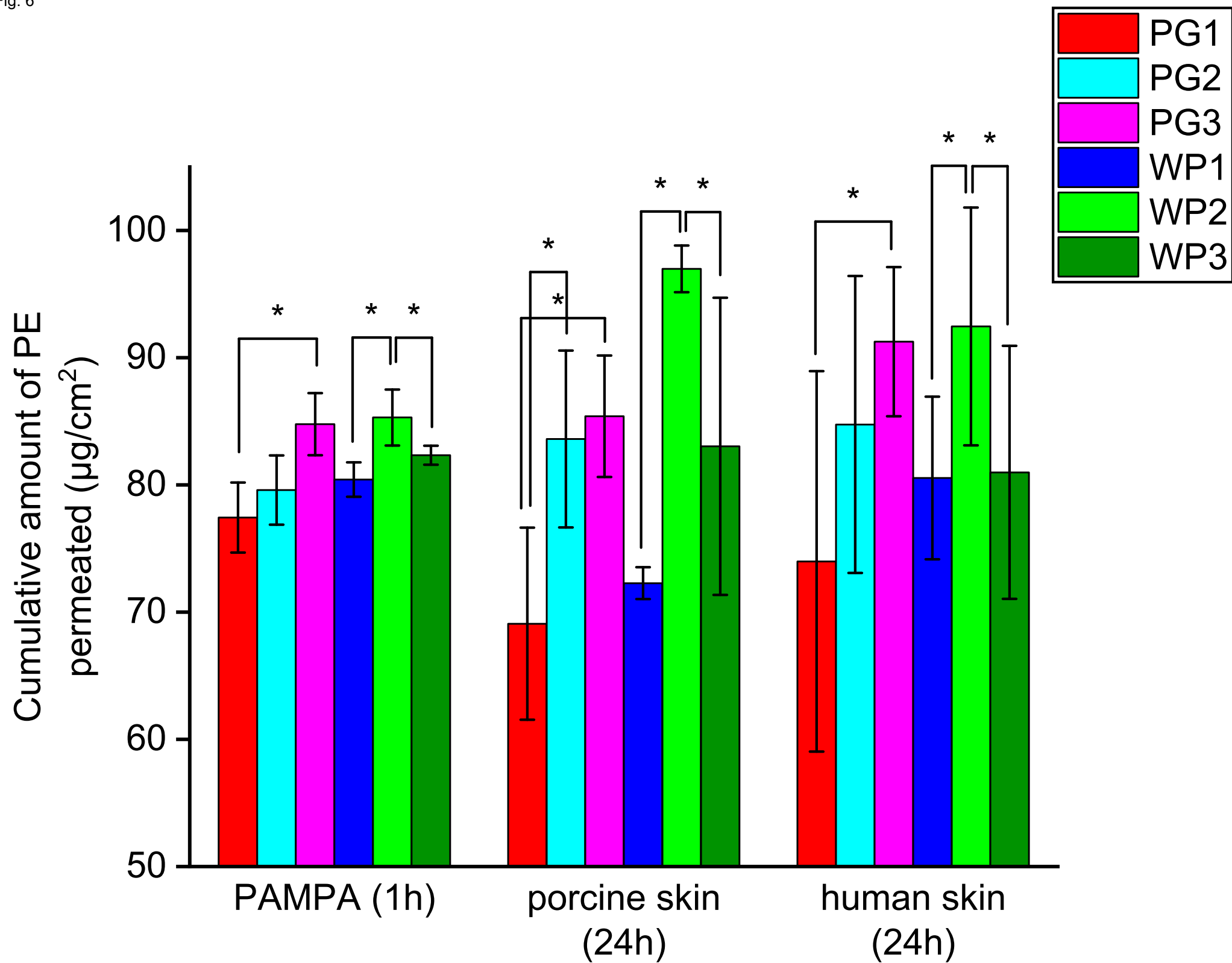
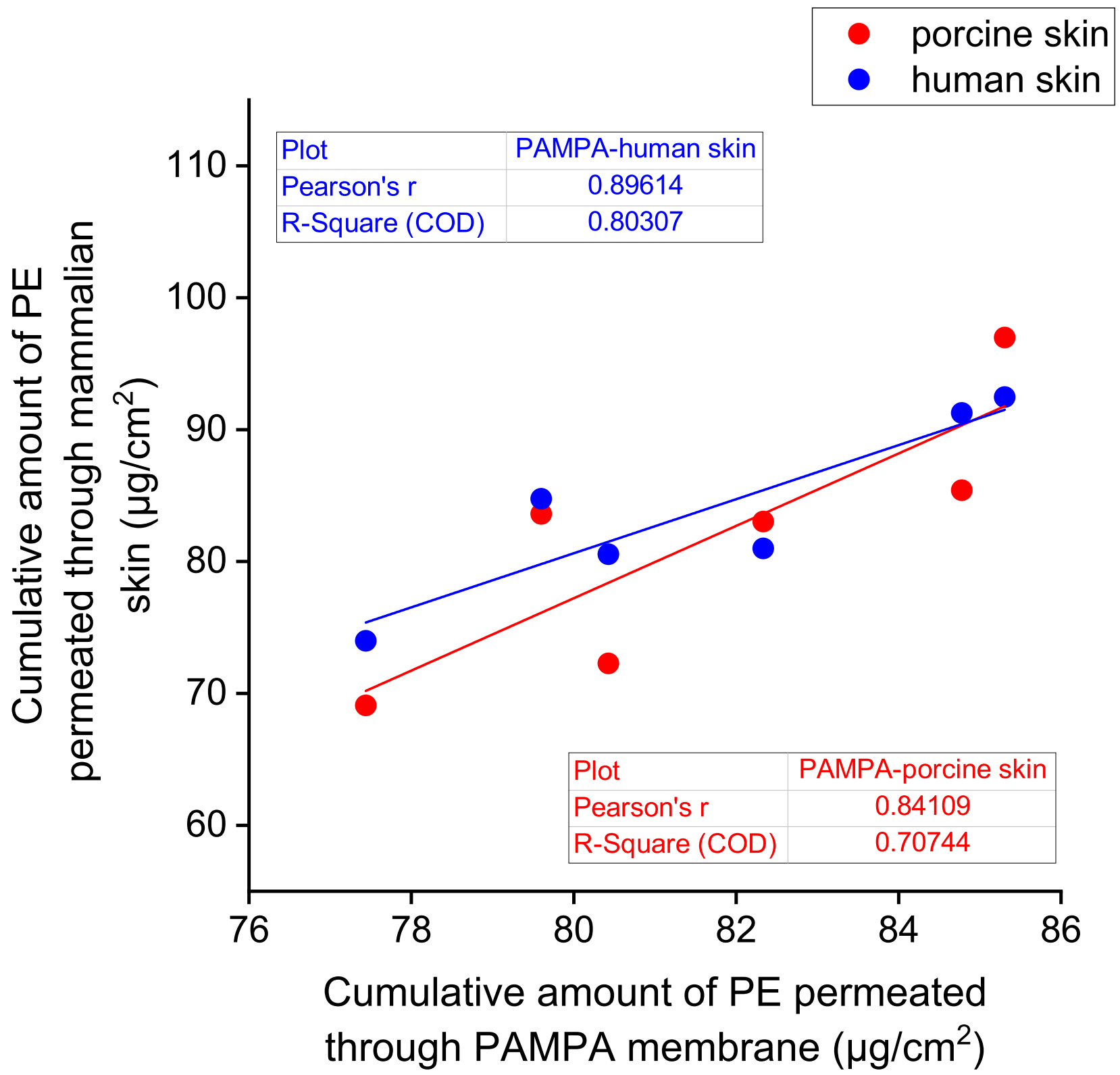


Fig. 7



CRedit authorship contribution statement

Annisa Rahma: Conceptualization, Methodology, Validation, Investigation, Formal analysis, Visualization, Writing – original draft. **Majella E. Lane:** Conceptualization, Resources, Supervision, Writing – review & editing. **Bálint Sinkó:** Conceptualization, Methodology, Formal analysis, Resources.